Ideal Gas Reference for Association and Dissociation Reactions: II. Kinetic Reference Potentials and Concentration Bias in Electrolysis

Tobias Binninger,[1, a)] Adrian Heinritz,[2] and Rhiyaad Mohamed[3, b)]

[1)] *ICGM, Univ Montpellier, CNRS, ENSCM, Montpellier, France*

[2)] *Electrochemistry Laboratory, Paul Scherrer Institut, 5232 Villigen, Switzerland*

[3)] *HySA/Catalysis Centre of Competence, Catalysis Institute, Department of Chemical Engineering, University of Cape Town, 7701, South Africa*

The ideal gas reference for association and dissociation reactions, developed in the first part of this series, is applied to electrochemical reactions. We obtain an ideal Nernst equation that quantifies the unspecific voltage contribution arising from an imbalance between the reactant and product concentrations of an electrochemical reaction for the given conditions. Subtracting this concentration bias from the equilibrium voltage/potential, we define the "kinetic reference voltage/potential" where the reactant and product states are "aligned" within the potential energy landscape of the system. The kinetic reference voltage/potential is a fundamental descriptor for a given electrochemical reaction, providing an intrinsic reference point which is most relevant in cases where the (standard) equilibrium voltage/potential is biased by large concentration differences between the reactant and product side. This is most dramatic for the case of water electrolysis, where the gaseous H_2 and O_2 product concentrations are several orders of magnitude smaller than the liquid water reactant concentration. The respective equilibrium voltage is strongly biased by the low H_2 and O_2 concentrations, although the latter do not directly influence the forward water splitting rate. The unbiased kinetic reference voltage agrees remarkably well with the experimentally observed onset of macroscopic water splitting rates. We further extend our analysis to the kinetic reference potentials of the hydrogen evolution reaction (HER), oxygen evolution reaction (OER), and lattice oxygen evolution reaction (LOER), providing an unconventional perspective on pH-dependent overpotentials, anticipated electrocatalysis improvements, and kinetic stabilization of electrocatalyst materials.

[a)]Electronic mail: tobias.binninger.science@gmx.de

[b)]Electronic mail: rhiyaad.mohamed@uct.ac.za

I. INTRODUCTION

The electrode potential E is the primary state variable of an electrochemical system because it provides facile control over the rate of electrochemical reactions. Consequently, the essential part of electrochemistry deals with the question at which rate a certain reaction proceeds at a given potential. The rate of a desired reaction should be maximized for an optimal efficiency of the process, which is often achieved by the utilization of an electrocatalyst. The rate of an unwanted degradation reaction should be minimized to enable long-term operation of an electrochemical device. Since only potential *differences* have a physical meaning, any analysis of an electrochemical process requires the specification of a reference potential. Typically, the electrode potential is expressed in terms of an overpotential $\eta = E - E_{\mathrm{eq}}$ with the "floating" equilibrium potential E_{eq} of the reaction *for the given conditions* as a reference. Alternatively, the relation between reaction kinetics and electrode potential can be described using the standard equilibrium potential $E_{\mathrm{eq}}^{\ominus}$ as a fixed reference. The following questions arise: Which reference potential is best suited for an assessment of the kinetics of an electrochemical reaction? At which potential can we decide whether the reaction reveals "fast" or "slow" kinetics?

In the following, we argue why neither E_{eq} nor $E_{\mathrm{eq}}^{\ominus}$ meet these criteria in general. This is best explained at the example of an elementary half-cell reaction $\mathrm{Red} \rightleftharpoons \mathrm{Ox} + \mathrm{e}^-$ assuming a Butler-Volmer relationship between the kinetic current density i_{kin} and the overpotential $\eta = E - E_{\mathrm{eq}}$,

$$i_{\mathrm{kin}} = i_0 \left[\exp\left(\frac{\alpha_{\mathrm{a}} F \eta}{RT} \right) - \exp\left(-\frac{\alpha_{\mathrm{c}} F \eta}{RT} \right) \right] \ , \tag{1}$$

with anodic and cathodic transfer coefficients α_{a} and α_{c}, respectively, fulfilling $\alpha_{\mathrm{a}} + \alpha_{\mathrm{c}} = 1$. The reaction velocity is quantified by the exchange current density i_0 that corresponds to the magnitude of the balanced kinetic currents of oxidation and reduction at $\eta = 0$. Therefore, i_0 is the quantity of interest when the kinetics of the reaction are investigated under different reaction conditions, e.g. concentrations, pH-value, or pressure. Changes in the concentrations c_{Ox} or c_{Red} produce a shift in the equilibrium potential E_{eq} via the Nernst equation

$$E_{\mathrm{eq}} = E_{\mathrm{eq}}^{\ominus} + \frac{RT}{zF} \log\left(\frac{c_{\mathrm{Ox}}/c_{\mathrm{Ox}}^{\ominus}}{c_{\mathrm{Red}}/c_{\mathrm{Red}}^{\ominus}} \right) \ , \tag{2}$$

where $c_{\mathrm{Ox}}^{\ominus}$ and $c_{\mathrm{Red}}^{\ominus}$ are the corresponding concentrations at standard conditions, and we neglected the activity coefficients for the sake of clarity. Consequently, it is often assumed that the primary effect of concentration changes is implicitly taken into account by using the overpotential scale, and the exchange current density i_0 would remain largely unaffected, at least to leading order. However, it is well established that the exchange current density itself strongly depends on the concentrations even for the most basic Butler-Volmer model[1],

$$i_0 = i_0^{\ominus} \left(\frac{c_{\mathrm{Red}}}{c_{\mathrm{Red}}^{\ominus}}\right)^{\alpha_{\mathrm{c}}} \left(\frac{c_{\mathrm{Ox}}}{c_{\mathrm{Ox}}^{\ominus}}\right)^{\alpha_{\mathrm{a}}} \tag{3}$$

with $i_0^{\ominus}$ being the exchange current density at standard concentrations. Consequently, to take into account the full concentration dependence of the kinetic current in Eq. (1), both the equilibrium potential, Eq. (2), and the exchange current density, Eq. (3), must be considered.

Inserting Eqs. (3) and (2) (with $z = 1$) into Eq. (1), we obtain

$$i_{\mathrm{kin}} = i_0^{\ominus} \left[\left(\frac{c_{\mathrm{Red}}}{c_{\mathrm{Red}}^{\ominus}}\right) \exp\left(\frac{\alpha_{\mathrm{a}} F}{RT}(E - E_{\mathrm{eq}}^{\ominus})\right) - \left(\frac{c_{\mathrm{Ox}}}{c_{\mathrm{Ox}}^{\ominus}}\right) \exp\left(-\frac{\alpha_{\mathrm{c}} F}{RT}(E - E_{\mathrm{eq}}^{\ominus})\right) \right] , \tag{4}$$

where we used $\alpha_{\mathrm{a}} + \alpha_{\mathrm{c}} = 1$. This form of the Butler-Volmer equation is precisely equivalent to Eq. (1), but now the electrode potential is given vs. the *fixed* standard equilibrium potential $E_{\mathrm{eq}}^{\ominus}$. We note that Eq. (4) must be regarded as the more fundamental version of the Butler-Volmer equation[2], and it typically represents the basis for the derivation of the overpotential version Eq. (1). As a great advantage, the concentration dependence is directly visible in Eq. (4). We simply recover the comprehensible behavior that the oxidation rate is proportional to the concentration of the reduced species, and vice versa for the reduction rate. In particular, on the fixed reference potential scale, the oxidation and reduction rates are *independent* of their respective product concentrations c_{Ox} and c_{Red}. This is what we expect from basic kinetic theory, where the forward and backward rates of a reaction $\mathrm{A} \rightleftarrows \mathrm{B}$ are given by $R_{\mathrm{f}} = k_{\mathrm{f}} c_{\mathrm{A}}$ and $R_{\mathrm{b}} = k_{\mathrm{b}} c_{\mathrm{B}}$, respectively, with certain rate constants $k_{\mathrm{f/b}}$. The use of the fixed reference potential scale thus appears superior to the overpotential scale, because the former enables to distinguish this fundamental concentration effect from other kinetic factors.

The situation is schematically visualized in Figure 1 showing the anodic branch, $i_{\mathrm{kin,a}} = i_0^{\ominus} \left(\frac{c_{\mathrm{Red}}}{c_{\mathrm{Red}}^{\ominus}}\right) \exp\left(\frac{\alpha_{\mathrm{a}} F}{RT}(E - E_{\mathrm{eq}}^{\ominus})\right)$, and cathodic branch, $i_{\mathrm{kin,c}} = -i_0^{\ominus} \left(\frac{c_{\mathrm{Ox}}}{c_{\mathrm{Ox}}^{\ominus}}\right) \exp\left(-\frac{\alpha_{\mathrm{c}} F}{RT}(E - E_{\mathrm{eq}}^{\ominus})\right)$, of the Butler-Volmer equation (4) on a fixed potential scale for two different concentrations of the oxidized species. The Nernst equilibrium potential E_{eq}, indicated by vertical lines

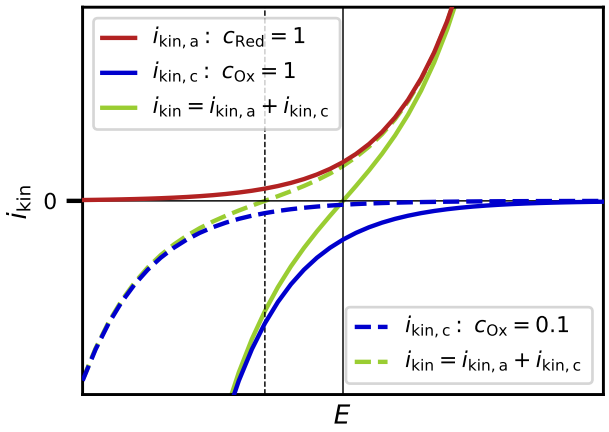

FIG. 1. Schematic plot of anodic, cathodic, and total kinetic currents according to the Butler-Volmer equation (4) vs. a fixed reference potential for two different concentrations of the oxidized species. The corresponding positions of the equilibrium potential are indicated by vertical lines.

where anodic and cathodic kinetic currents are balanced, shifts negative due to the decreased current magnitude of the cathodic branch at a decreased value of c_{Ox}, in agreement with the Nernst equation (2). Since the anodic branch is unaffected by c_{Ox}, the actual exchange current density i_0, i.e. the balanced current magnitude of anodic and cathodic branches at E_{eq}, gets decreased with the shift in E_{eq}, which illustrates the origin of the concentration dependence of i_0 given in Eq. (3). Furthermore, the total kinetic current $i_{\mathrm{kin}} = i_{\mathrm{kin,a}} + i_{\mathrm{kin,c}}$ of Eq. (4) converges to the anodic branch at large potentials and to the cathodic branch at small potentials. As a result, the influence of the concentration c_{Ox} on the total kinetic current becomes negligible at sufficiently large potentials and the actual position of the equilibrium potential E_{eq} becomes irrelevant.

The fact that the fixed potential scale is better suited for kinetic analysis than the overpotential remains true also for multistep reactions. For example, the same reasoning was used to explain why the rate of the oxygen evolution reaction (OER) was observed to be rather unaffected by the presence or absence of oxygen during the experiment[3]. The oxygen concentration primarily acts on the backward reaction, i.e. the oxygen reduction reaction (ORR), which is negligible at potentials relevant for the OER. According to the same argument, polarization curves of water electrolyzers would be expected to be largely insensitive towards the oxygen pressure under operation, especially at high current densities. This insight appears to be mostly neglected in the present literature when discussing the observed

vs. expected influence of high-pressure operation[4].

Having established that the "floating" equilibrium potential E_{eq} does not, in general, represent a reliable reference for kinetic analysis, we argue that even the fixed standard equilibrium potential $E_{\mathrm{eq}}^{\ominus}$ does not fulfill such criterion. The choice of the standard pressure of 1 bar for gaseous species and concentrations of $1\,\mathrm{mol\,L^{-1}}$ for dissolved species is, to a certain extent, arbitrary and fixed by convention. Moreover, this choice is ambiguous for dissolved gases. For hydrogen and oxygen, e.g., at a standard pressure of $p^{\ominus} = 1\,\mathrm{bar}$ and $T = 25°\mathrm{C}$, the corresponding saturation concentrations of hydrogen and oxygen molecules dissolved in water are $c_{\mathrm{H_2,aq}}^{\ominus} = 0.771 \times 10^{-3}\,\mathrm{mol\,L^{-1}}$ and $c_{\mathrm{O_2,aq}}^{\ominus} = 1.252 \times 10^{-3}\,\mathrm{mol\,L^{-1}}$, respectively[5,6]. However, for dissolved H_2 and O_2 one could argue that the standard concentration of $1\,\mathrm{mol\,L^{-1}}$ should rather be used, in particular since only dissolved molecules can participate in an electrochemical reaction step. Redefining the standard concentrations would shift $E_{\mathrm{eq}}^{\ominus}$ according to the Nernst equation (2) and alter the corresponding exchange current density $i_0^{\ominus}$ according to Eq. (3). Therefore, $E_{\mathrm{eq}}^{\ominus}$ does not represent an intrinsic reference point on the potential axis for a given reaction. In particular, it would be incorrect to assume that any given electrochemical reaction could proceed at a significant rate in the potential range around $E_{\mathrm{eq}}^{\ominus}$, if only the optimal catalyst were available.

We exemplify this aspect for the OER, $2\,H_2O \rightarrow O_2 + 4\,H^+ + 4\,e^-$, with a standard equilibrium potential $E_{\mathrm{eq}}^{\ominus} = 1.229\,\mathrm{V_{SHE}}$ corresponding to $p_{\mathrm{O_2}}^{\ominus} = 1\,\mathrm{bar}$. An electrocatalyst material that would enable significant OER rates close to $E_{\mathrm{eq}}^{\ominus}$ could be regarded as the "philosophers' stone" in electrocatalysis. But why should this be possible at all, why should such "philosophers' stone" electrocatalyst exist? Whereas the standard equilibrium potential strongly depends on the choice of $p_{\mathrm{O_2}}^{\ominus}$, the actual OER rate is largely independent of the oxygen partial pressure, as discussed above and confirmed by experiment. The particular value of $p_{\mathrm{O_2}}^{\ominus} = 1\,\mathrm{bar}$ has no relevance for the OER rate observed at a certain *fixed* potential on a given catalyst. Hence, it is not clear *a priori* why significant OER rates should be possible close to $1.229\,\mathrm{V_{SHE}}$ even on an "ideal" catalyst (the meaning of which will be discussed later on). In fact, the standard pressure of 1 bar simply corresponds to an average atmospheric pressure on Earth. Imagine some intelligent species had evolved on planet Pluto and defined a different standard pressure of $p_{\mathrm{O_2}}^{\oplus} = 10^{-5}\,\mathrm{bar}$ according to the local atmospheric conditions[7]. They might now search for an ideal catalyst to enable the OER at their standard equilibrium potential $E_{\mathrm{eq}}^{\oplus} = E_{\mathrm{eq}}^{\ominus} + \frac{RT}{4F}\,\log\left(p_{\mathrm{O_2}}^{\oplus}/p_{\mathrm{O_2}}^{\ominus}\right) = 1.155\,\mathrm{V_{SHE}}$.

Now, would an ideal catalyst provide an onset potential for macroscopic OER rates around our standard equilibrium potential of $1.229\,\mathrm{V_{SHE}}$, their standard equilibrium potential of $1.155\,\mathrm{V_{SHE}}$, or none of them?

After this discussion, we seem to be left without an intrinsic point of orientation along the potential axis. In the following, we present an approach to close this gap and we use the ideal gas reference for chemical association/dissociation reactions, developed in Part I. of the present series[8], to define the *kinetic reference potential* for electrochemical reactions. Its usefulness and physical meaning become particularly clear when applied to electrolysis reactions involving the transition between the liquid and gaseous phase. Finally, our discussion offers a new perspective on the pH-effect in the kinetics of HER and OER, and the kinetic stabilization of certain metal oxide electrocatalysts during OER.

II. THEORY

A. Ideal and excess Gibbs free energy of reaction

In Part I. of the present series[8], we developed an ideal gas reference for association and dissociation reactions, the most relevant findings of which will be summarized in this section. We introduced a straightforward definition of molecules simply based on the distance between the atomic constituents. If two atoms are closer than some critical distance ℓ_{ch}, we consider them as being part of one molecular entity. If their distance is larger than ℓ_{ch}, we consider them as being separate. This definition is in agreement with IUPAC terminology[9]. Importantly, it provides a notion of molecules consisting of non-interacting constituents, which we used to study equilibria and kinetics of association and dissociation reactions in mixtures of ideal gases, yielding an ideal law of mass action and ideal kinetic rate equations. The ideal gas reference is equally obtained in the limit of an entirely flat potential energy "landscape" of the system. Therefore, the difference between a real association/dissociation reaction and the corresponding ideal gas reference originates from the system-specific unevenness of the potential energy surface. Consequently, we defined the *excess* equilibrium and rate constants to quantify these system-specific effects.

Considering a general association/dissociation reaction $\sum_i \rho_i \,\mathrm{R}_i \rightleftharpoons \sum_j \pi_j \,\mathrm{P}_j$ with reactant species R_i, product species P_j, and stoichiometric coefficients ρ_i and π_j, we obtained

an ideal Gibbs free energy of reaction

$$\Delta_{\mathrm{r}}G_{\mathrm{id}} \;=\; k_{\mathrm{B}}T\,\ln\left(\frac{1}{g_{\mathrm{r}}}\,\frac{\prod_j \left(c_{\mathrm{P}_j}/c_*\right)^{\pi_j}}{\prod_i \left(c_{\mathrm{R}_i}/c_*\right)^{\rho_i}}\right) \tag{5}$$

as a function of the reactant and product concentrations c_{R_i} and c_{P_j}, respectively. Here, $g_{\mathrm{r}} = \prod_i \left(g_{\mathrm{R}_i}\right)^{\rho_i} / \prod_j \left(g_{\mathrm{P}_j}\right)^{\pi_j}$ is an overall combinatorial factor of the reaction with $g_{\mathrm{R}_i} = (\alpha_i!\,\beta_i!\,\gamma_i!)$ and $g_{\mathrm{P}_j} = (\alpha_j!\,\beta_j!\,\gamma_j!)$ being combinatorial factors for each of the reactants $\mathrm{R}_i = (\mathrm{A}_{\alpha_i}\mathrm{B}_{\beta_i}\mathrm{C}_{\gamma_i})$ and products $\mathrm{P}_j = \left(\mathrm{A}_{\alpha_j}\mathrm{B}_{\beta_j}\mathrm{C}_{\gamma_j}\right)$ accounting for the indistinguishability of atomic constituents of some general types A, B, C. Generalization to more than three atom types is straightforward. We note that g_{r} is generally of order unity and thus rather insignificant for the value of $\Delta_{\mathrm{r}}G_{\mathrm{id}}$. Most importantly, in Eq. (5) the concentrations of reactants and products are naturally referenced to the concentration $c_* = c_{\mathrm{ch}}\,e^{-(c_{\mathrm{tot}}/c_{\mathrm{ch}})}$, where $c_{\mathrm{ch}} = 1/V_{\mathrm{ch}}$ is the *chemical reference concentration* that is equal to the *inverse of the molecular volume* $V_{\mathrm{ch}} = (4/3)\pi\ell_{\mathrm{ch}}^3$ of radius ℓ_{ch}. The factor $e^{-(c_{\mathrm{tot}}/c_{\mathrm{ch}})}$ corresponds to the probability of *not* finding any chemical entity within a given volume element V_{ch}, where c_{tot} is the sum of concentrations of all chemical species present in the system. Therefore, c_* can be interpreted as the concentration of "unoccupied" volume elements V_{ch}. In the limit of a dilute system, we simply have $c_* \approx c_{\mathrm{ch}}$.

We emphasize that c_{ch} defines an intrinsic chemical concentration scale that is determined by the molecular size. Whereas various definitions of the size of a molecule exist, such details are of little importance as long as they differ only by factors of order unity that have an insignificant effect on the value of $\Delta_{\mathrm{r}}G_{\mathrm{id}}$ and the kinetic reference potential to be defined below. For the same reason, a system consisting of different molecular species can be treated by only one effective c_{ch} being equal to the inverse of an average molecular volume of the system. These aspects will be further clarified by the examples in the Results and Discussion section.

We then defined the excess Gibbs free energy of reaction $\Delta_{\mathrm{r}}G_{\mathrm{xs}} = \Delta_{\mathrm{r}}G - \Delta_{\mathrm{r}}G_{\mathrm{id}}$ of the real system to quantify the difference between the actual Gibbs free energy of reaction $\Delta_{\mathrm{r}}G$ and the corresponding ideal gas reference $\Delta_{\mathrm{r}}G_{\mathrm{id}}$. The actual Gibbs free energy of reaction can be written in the form

$$\Delta_{\mathrm{r}}G = \Delta_{\mathrm{r}}G^{\ominus} + k_{\mathrm{B}}T\,\ln\left(\frac{\prod_j \left(a_{\mathrm{P}_j}\right)^{\pi_j}}{\prod_i \left(a_{\mathrm{R}_i}\right)^{\rho_i}}\right) \tag{6}$$

with the standard Gibbs free energy of reaction $\Delta_\mathrm{r}G^\ominus = \sum_j \pi_j \mu^\ominus_{\mathrm{P}_j} - \sum_i \rho_i \mu^\ominus_{\mathrm{R}_i}$ and activities a_{R_i} and a_{P_j} of reactants and products, respectively. Using Eqs. (5) and (6), the excess Gibbs free energy of reaction reads

$$\Delta_\mathrm{r}G_\mathrm{xs} \;=\; \Delta_\mathrm{r}G^\ominus + k_\mathrm{B}T\,\ln\left(g_\mathrm{r}\right) + k_\mathrm{B}T\,\ln\left(\frac{\prod_j \left(c_*/c^\ominus_{\mathrm{P}_j}\right)^{\pi_j}}{\prod_i \left(c_*/c^\ominus_{\mathrm{R}_i}\right)^{\rho_i}}\right) + k_\mathrm{B}T\,\ln\left(\Gamma_\mathrm{c,r}\right)\;, \qquad (7)$$

where we used the form $a = \gamma_\mathrm{c}\,(c/c^\ominus)$ for each of the activities with the concentration-based activity coefficient γ_c, and $\Gamma_\mathrm{c,r} = \prod_j \left(\gamma_{\mathrm{c,P}_j}\right)^{\pi_j} / \prod_i \left(\gamma_{\mathrm{c,R}_i}\right)^{\rho_i}$ is the corresponding quotient of activity coefficients of the reaction. Although Eq. (7) involves standard state ($\ominus$) quantities, it is actually independent of the choice of the standard reference concentrations $c^\ominus_{\mathrm{R}_i}$ and $c^\ominus_{\mathrm{P}_j}$, because respective dependencies of the individual terms mutually get cancelled in Eq. (7). Also, the excess Gibbs free energy of reaction is only weakly dependent on the actual concentrations through the quotient of activity coefficients $\Gamma_\mathrm{c,r}$.

B. Kinetic reference potentials and voltages

As discussed in Part I. of our series[8], the excess quantities measure those effects that result from the system-specific shape of the potential energy surface in the system's configuration space. All unspecific concentration effects that simply result from particle number statistics are captured by the ideal gas reference. Therefore, the excess Gibbs free energy of reaction quantifies the alignment of reactants and products within the potential energy landscape. If $\Delta_\mathrm{r}G_\mathrm{xs}$ is equal to zero, the reactants and products can be regarded to be aligned at the same "height" in potential energy. Importantly, in contrast to the enthalpy of reaction $\Delta_\mathrm{r}H$, the excess Gibbs free energy of reaction includes those entropic contributions that result from the unevenness of the potential energy surface. Only the unspecific entropic contribution due to particle number combinatorics is removed by subtracting the ideal gas reference.

We therefore consider the excess Gibbs free energy of reaction $\Delta_\mathrm{r}G_\mathrm{xs}$ as the natural basis to define intrinsic reference potentials and voltages for electrochemical half-cell and full-cell reactions, respectively. These are consequently denoted *excess potential* E_xs and *excess voltage* U_xs, respectively. Alternatively, following from their physical meaning discussed below, it appears justified to use the terms *kinetic reference potential* E_kin and *kinetic reference voltage* U_kin interchangeably for E_xs and U_xs, respectively.

If the general association/dissociation reaction discussed above is the overall redox reaction of a full electrochemical cell that involves the exchange of z electrons, the corresponding ideal Gibbs free energy of reaction of Eq. (5) defines an *ideal equilibrium voltage* $U_{\mathrm{id}} = \Delta_{\mathrm{r}} G_{\mathrm{id}}/ze$,

$$U_{\mathrm{id}} \;=\; \frac{RT}{zF}\,\ln\left(\frac{1}{g_{\mathrm{r}}}\,\frac{\prod_j \left(c_{\mathrm{P}_j}/c_*\right)^{\pi_j}}{\prod_i \left(c_{\mathrm{R}_i}/c_*\right)^{\rho_i}}\right)\;, \tag{8}$$

where we used $k_{\mathrm{B}}T/e = RT/F$. We note that this equation can be regarded as an *ideal Nernst equation*, which is reduced to the logarithm term where all concentrations are intrinsically referenced to the concentration c_*.

We now define the *kinetic reference voltage* of the same reaction by $U_{\mathrm{kin}} = \Delta_{\mathrm{r}} G_{\mathrm{xs}}/ze$. The defining relation $\Delta_{\mathrm{r}} G_{\mathrm{xs}} = \Delta_{\mathrm{r}} G - \Delta_{\mathrm{r}} G_{\mathrm{id}}$ yields $U_{\mathrm{kin}} = U_{\mathrm{eq}} - U_{\mathrm{id}}$, so the kinetic reference voltage quantifies the difference between the actual equilibrium voltage $U_{\mathrm{eq}} = \Delta_{\mathrm{r}} G/ze$ and the corresponding ideal equilibrium voltage. Inserting Eq. (8), we obtain

$$U_{\mathrm{kin}} \;=\; U_{\mathrm{eq}} + \frac{RT}{zF}\,\ln\left(g_{\mathrm{r}}\right) + \frac{RT}{zF}\,\ln\left(\frac{\prod_j \left(c_*/c_{\mathrm{P}_j}\right)^{\pi_j}}{\prod_i \left(c_*/c_{\mathrm{R}_i}\right)^{\rho_i}}\right)\;. \tag{9}$$

Here, U_{kin} is related to the equilibrium voltage U_{eq} and concentrations c_{R_i} and c_{P_j} for the given conditions. It can equivalently be expressed in terms of the standard equilibrium voltage $U^{\ominus}_{\mathrm{eq}} = \Delta_{\mathrm{r}} G^{\ominus}/ze$ and the corresponding standard state concentrations $c^{\ominus}_{\mathrm{R}_i}$ and $c^{\ominus}_{\mathrm{P}_j}$. Using Eq. (7), we find

$$U_{\mathrm{kin}} \;=\; U^{\ominus}_{\mathrm{eq}} + \frac{RT}{zF}\,\ln\left(g_{\mathrm{r}}\right) + \frac{RT}{zF}\,\ln\left(\frac{\prod_j \left(c_*/c^{\ominus}_{\mathrm{P}_j}\right)^{\pi_j}}{\prod_i \left(c_*/c^{\ominus}_{\mathrm{R}_i}\right)^{\rho_i}}\right) + \frac{RT}{zF}\,\ln\left(\Gamma_{\mathrm{c,r}}\right)\;. \tag{10}$$

The difference between the kinetic reference voltage, or excess voltage, U_{kin} and the actual equilibrium voltage U_{eq} defines an *excess overvoltage* $\eta_{\mathrm{xs}} = U_{\mathrm{kin}} - U_{\mathrm{eq}} = -U_{\mathrm{id}}$ that is equal to the negative of the ideal equilibrium voltage.

Likewise, for a general half-cell reaction $\sum_i \rho_i \,\mathrm{Red}_i \rightleftharpoons \sum_j \pi_j \,\mathrm{Ox}_j + z\,\mathrm{e}^-$, we define the *kinetic reference potential*

$$E_{\mathrm{kin}} \;=\; E_{\mathrm{eq}} + \frac{RT}{zF}\,\ln\left(g_{\mathrm{r}}\right) + \frac{RT}{zF}\,\ln\left(\frac{\prod_j \left(c_*/c_{\mathrm{Ox}_j}\right)^{\pi_j}}{\prod_i \left(c_*/c_{\mathrm{Red}_i}\right)^{\rho_i}}\right)\;, \tag{11}$$

written versus the actual equilibrium potential E_{eq} for the given concentrations c_{Ox_j} and

c_{Red_i}. Equivalently, we can express E_{kin} in terms of the standard equilibrium potential $E_{\mathrm{eq}}^{\ominus}$,

$$E_{\mathrm{kin}} \;=\; E_{\mathrm{eq}}^{\ominus} + \frac{RT}{zF}\,\ln\left(g_{\mathrm{r}}\right) + \frac{RT}{zF}\,\ln\left(\frac{\prod_j \left(c_*/c_{\mathrm{Ox}_j}^{\ominus}\right)^{\pi_j}}{\prod_i \left(c_*/c_{\mathrm{Red}_i}^{\ominus}\right)^{\rho_i}}\right) + \frac{RT}{zF}\,\ln\left(\Gamma_{\mathrm{c,r}}\right)\;, \tag{12}$$

where $c_{\mathrm{Ox}_j}^{\ominus}$ and $c_{\mathrm{Red}_i}^{\ominus}$ are the concentrations at the standard state defined for each of the species on the oxidized and reduced side of the reaction equation, respectively. The difference between the kinetic reference potential, or excess potential, E_{kin} and the actual equilibrium potential E_{eq} defines an *excess overpotential* $\eta_{\mathrm{xs}} = E_{\mathrm{kin}} - E_{\mathrm{eq}}$, for which we obtain from Eq. (11)

$$\eta_{\mathrm{xs}} \;=\; \frac{RT}{zF}\,\ln\left(g_{\mathrm{r}}\right) + \frac{RT}{zF}\,\ln\left(\frac{\prod_j \left(c_*/c_{\mathrm{Ox}_j}\right)^{\pi_j}}{\prod_i \left(c_*/c_{\mathrm{Red}_i}\right)^{\rho_i}}\right)\;. \tag{13}$$

Physical meaning. The ideal equilibrium voltage of Eq. (8) is zero under the condition

$$\frac{1}{g_{\mathrm{r}}}\,\frac{\prod_j \left(c_{\mathrm{P}_j}\right)^{\pi_j}}{\prod_i \left(c_{\mathrm{R}_i}\right)^{\rho_i}}\,\frac{\left(c_*\right)^{\sum_i \rho_i}}{\left(c_*\right)^{\sum_j \pi_j}} \;=\; 1\;, \tag{14}$$

which is simply the ideal law of mass action derived in Part I. of this series. This condition characterizes the dynamic equilibrium within the ideal gas framework, where the balance between forward and backward rates of the reaction is purely determined by the balance in particle number statistics between the reactants and products, expressed by the corresponding concentration factors. We therefore term Eq. (14) the *condition of balanced concentrations*, which essentially corresponds to the equality of the stoichiometric product of concentrations between the reactant and product side of the reaction equation. For reactions with different total stoichiometries on both sides, the number of concentration factors is adjusted by an appropriate power of the concentration c_*.

If the reactant and product concentrations are unbalanced, meaning that they do not fulfill Eq. (14), the corresponding ideal equilibrium voltage of Eq. (8) is non-zero. U_{id} therefore quantifies that contribution to the actual equilibrium voltage of an electrochemical reaction that simply results from an imbalance between the actual reactant and product concentrations. This "concentration bias voltage" is independent of the shape of the potential energy landscape and therefore *unspecific*. The unbiased kinetic reference voltage $U_{\mathrm{kin}} = U_{\mathrm{eq}} - U_{\mathrm{id}}$ then represents the intrinsic *system-specific* part of the equilibrium voltage, and likewise for the kinetic reference potential E_{kin} of half-cell reactions. Consequently, U_{kin} and E_{kin} can be

interpreted as the equilibrium voltage and potential, respectively, at conditions of balanced reactant and product concentrations according to Eq. (14).

We discuss a complementary perspective on the physical meaning of E_{kin} and U_{kin}. From the meaning of the excess Gibbs free energy of reaction, discussed above and in Part I. of this series, it becomes clear that E_{kin} and U_{kin} correspond to the half-cell potential and full-cell voltage, respectively, where the reactant and product side of a given reaction are aligned within the potential energy surface of the system. This means that *the system-specific potential energy contributions to the Gibbs free energies of reactants and products are equal* at the kinetic reference potential/voltage. In contrast to the actual equilibrium potential and voltage, E_{kin} and U_{kin} are corrected for those Gibbs free energy differences that simply result from an imbalance between the reactant and product concentrations, as discussed above. Therefore, E_{kin} and U_{kin} allow to distinguish "intrinsic" effects due to the system-specific potential energy landscape from unspecific concentration effects that are captured by the ideal gas reference. We therefore regard the kinetic reference potential E_{kin} as an intrinsic point of orientation along the potential axis for the kinetic analysis of a given electrochemical reaction. The question at which rate an electrochemical reaction could be expected to proceed at E_{kin} under ideal conditions, i.e. which magnitude of the corresponding current density could be expected in presence of an ideal catalyst, will be addressed further below.

III. RESULTS AND DISCUSSION

The definition and meaningfulness of kinetic reference potentials/voltages is exemplified for a number of electrochemical reactions in the following. Table I gives an overview of the corresponding standard equilibrium potentials/voltages and kinetic reference potentials/voltages at $T = 25°\mathrm{C}$. The relevance of E_{kin} and U_{kin} is most pronounced for reactions that involve significant changes in concentration between the reactant and product side. This is the case, e.g., in water electrolysis that involves the transition from a condensed liquid reactant to gaseous products.

Reaction	Equation	$E^{\ominus}_{\mathrm{eq}}$ | $U^{\ominus}_{\mathrm{eq}}$	E_{kin} | U_{kin}
Water electrolysis	$2\,H_2O \rightleftharpoons 2\,H_2 + O_2$	1.229 V	1.437 V
HER acidic	$2\,H^+ + 2\,e^- \rightleftharpoons H_2$	0.0 $V_{RHE}^{pH\,0}$	−0.032 $V_{RHE}^{pH\,0}$
HER alkaline	$2\,H_2O + 2\,e^- \rightleftharpoons H_2 + 2\,OH^-$	0.0 $V_{RHE}^{pH\,14}$	−0.256 $V_{RHE}^{pH\,14}$
OER acidic	$2\,H_2O \rightleftharpoons O_2 + 4\,H^+ + 4\,e^-$	1.229 $V_{RHE}^{pH\,0}$	1.405 $V_{RHE}^{pH\,0}$
OER alkaline	$4\,OH^- \rightleftharpoons O_2 + 2\,H_2O + 4\,e^-$	1.229 $V_{RHE}^{pH\,14}$	1.181 $V_{RHE}^{pH\,14}$
LOER IrO_2	$IrO_2 \rightleftharpoons Ir^{3+}_{aq} + O_2 + 3\,e^-$	1.561 $V_{RHE}^{pH\,0}$	1.686 $V_{RHE}^{pH\,0}$
LOER(I) CoOOH	$CoOOH + OH^- \rightleftharpoons Co^{3+}_{aq} + O_2 + H_2O + 4\,e^-$	1.968 $V_{RHE}^{pH\,14}$	2.032 $V_{RHE}^{pH\,14}$
LOER(II) CoOOH	$CoOOH + OH^- \rightleftharpoons Co^{2+}_{aq} + O_2 + H_2O + 3\,e^-$	1.694 $V_{RHE}^{pH\,14}$	1.780 $V_{RHE}^{pH\,14}$

TABLE I. Standard equilibrium potentials $E^{\ominus}_{\mathrm{eq}}$ and kinetic reference potentials E_{kin} at $T = 25°\mathrm{C}$ of the various electrochemical reactions discussed. For the overall water electrolysis reaction, values refer to the standard equilibrium voltage $U^{\ominus}_{\mathrm{eq}}$ and kinetic reference voltage U_{kin}.

A. Unimolecular electrochemical reactions

We first consider a simple electrochemical electron-transfer reaction $\mathrm{Red} \rightleftharpoons \mathrm{Ox} + \mathrm{e}^-$ for a single species in solution, so with Red and Ox corresponding to one solvated ion or complex in a reduced and oxidized state, respectively. Because the reacting species only changes its oxidation state but not its chemical composition, we have $g_{\mathrm{r}} = 1$. Furthermore, the same standard concentration applies to the reduced and oxidized species, $c^{\ominus}_{\mathrm{Red}} = c^{\ominus}_{\mathrm{Ox}} = 1\,\mathrm{mol\,L^{-1}}$. Therefore, both the second and the third term on the right-hand side of Eq. (12) are zero and the kinetic reference potential is given by

$$E_{\mathrm{kin}} \;=\; E^{\ominus}_{\mathrm{eq}} + \frac{RT}{zF}\,\ln\left(\Gamma_{\mathrm{c,r}}\right)\;. \tag{15}$$

In a dilute solution, the quotient of activity coefficients $\Gamma_{\mathrm{c,r}} = \gamma_{\mathrm{c,Ox}}/\gamma_{\mathrm{c,Red}} \approx 1$ is approximately equal to one, and E_{kin} turns to $E^{\ominus}_{\mathrm{eq}}$. Therefore, the kinetic reference potential of a simple electrochemical redox couple is essentially equal to the corresponding standard equilibrium potential. This results from the fact that the standard state of reactants and products fulfills the condition of balanced concentrations, $c^{\ominus}_{\mathrm{Red}} = c^{\ominus}_{\mathrm{Ox}}$.

B. Water electrolysis

An entirely different situation is found for the water electrolysis reaction, $2\,H_2O \rightleftharpoons 2\,H_2 + O_2$. Firstly, the total stoichiometries of both sides of the reaction differ, namely two molecules of water get split to form a total of three product molecules. Secondly, the standard state concentration of liquid water[10] at $T = 25°C$ is $c^{\ominus}_{H_2O,\ell} = 55.34\,\mathrm{mol\,L^{-1}}$. In contrast, for the hydrogen and oxygen product molecules dissolved in water, the saturation concentrations at a standard pressure of $p^{\ominus} = 1\,\mathrm{bar}$ are $c^{\ominus}_{H_2,aq} = 0.771 \times 10^{-3}\,\mathrm{mol\,L^{-1}}$ and $c^{\ominus}_{O_2,aq} = 1.252 \times 10^{-3}\,\mathrm{mol\,L^{-1}}$, respectively[5,6]. Thus, the reactant and product concentrations are extremely unbalanced at standard state. Whereas the standard equilibrium voltage[11] $U^{\ominus}_{eq} = 1.229\,V$ of the water electrolysis reaction is strongly biased by this imbalance, the low H_2 and O_2 product concentrations do not directly influence the forward rate of the water splitting reaction, as discussed in the Introduction. Therefore, $U^{\ominus}_{eq}$ does not represent an intrinsic reference for an analysis of the reaction kinetics of electrolytic water splitting.

According to Eq. (10), the kinetic reference voltage of the water electrolysis reaction, with $z = 4$, reads

$$U_{kin} = U^{\ominus}_{eq} + \frac{RT}{4F}\,\ln\left(g_r\right) + \frac{RT}{4F}\,\ln\left(\frac{\left(c^{\ominus}_{H_2O,\ell}\right)^2\left(c_*\right)}{\left(c^{\ominus}_{H_2,aq}\right)^2\left(c^{\ominus}_{O_2,aq}\right)}\right) + \frac{RT}{4F}\,\ln\left(\Gamma_{c,r}\right)\ . \tag{16}$$

The combinatorial factors of the involved species are $g_{H_2O} = 2! = 2$, $g_{H_2} = 2! = 2$, and $g_{O_2} = 2! = 2$, and thus the overall combinatorial factor of the reaction $g_r = g^2_{H_2O}/\left(g^2_{H_2}\,g_{O_2}\right) = 1/2$. We note that the corresponding term in Eq. (16) only accounts for $\approx -0.004\,V$ at room temperature. If the experimental conditions are close to the standard conditions, the quotient of activity coefficients $\Gamma_{c,r} = \left(\gamma_{c,H_2}\right)^2\left(\gamma_{c,O_2}\right)/\left(\gamma_{c,H_2O}\right)^2 \approx 1$ is approximately equal to one, and the respective term in Eq. (16) is negligible.

To assess the remaining term, we must determine $c_* = c_{ch}\,e^{-(c_{tot}/c_{ch})}$. As discussed in Part I. of this series, the chemical reference concentration $c_{ch} = 1/V_{ch}$ is equal to the inverse of a molecular volume. We quantify the latter by the spherical volume $V_{ch} = (4/3)\pi\ell^3_{ch}$, where ℓ_{ch} is the critical distance between the dissociating constituent atoms that separates the molecular state from the dissociated state. For the case of water splitting, a reasonable choice of ℓ_{ch} would thus be some value in between the O–H bond length of $\approx 1\,Å$ within a water molecule and the O$\cdots$H hydrogen bond length of $\approx 2\,Å$ between adjacent water molecules. An intermediate value of $\ell_{ch} = 1.5\,Å$ would yield $c_{ch} = 117.5\,\mathrm{mol\,L^{-1}}$. Furthermore approxi-

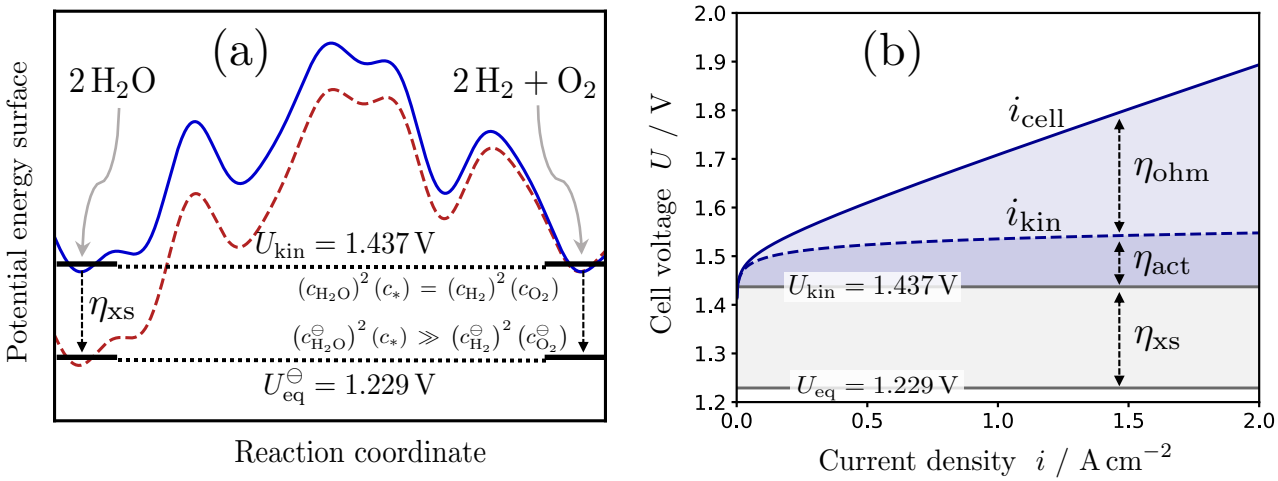

FIG. 2. (a) Schematic representation of the potential energy surface (PES) along a hypothetical reaction coordinate parametrizing the entire electrolytic water splitting pathway including both half-cell reactions of OER and HER. The solid blue PES corresponds to a cell voltage equal to $U_{\mathrm{kin}} = 1.437\,\mathrm{V}$, whereas the dashed red PES illustrates the situation at $U^{\ominus}_{\mathrm{eq}} = 1.229\,\mathrm{V}$. The corresponding Gibbs free energies are indicated by solid horizontal bars for balanced concentration conditions (top) and standard conditions (bottom). (b) Typical polarization curve of a proton-exchange membrane (PEM) water electrolyzer and partitioning of the cell voltage into contributions of the ohmic overvoltage $\eta_{\mathrm{ohm}} = RI_{\mathrm{cell}}$, the redefined activation overvoltage η_{act}, and the excess overvoltage η_{xs}. In the plotted current density range, overvoltage contributions of mass-transport limitations are generally negligible and therefore not indicated.

mating the total concentration of chemical species present by $c_{\mathrm{tot}} \approx c^{\ominus}_{\mathrm{H_2O},\ell} = 55.34\,\mathrm{mol\,L^{-1}}$, we obtain an estimation $c_* = c_{\mathrm{ch}}\, e^{-(c_{\mathrm{tot}}/c_{\mathrm{ch}})} \approx 73.33\,\mathrm{mol\,L^{-1}}$. We note that this value is of the order of the liquid water concentration of $55.34\,\mathrm{mol\,L^{-1}}$. At this point, we simply *define* $c_* = c^{\ominus}_{\mathrm{H_2O},\ell}$ to be equal to the concentration of liquid water. The amount of arbitrariness introduced by this choice is insignificant. The difference between $73.33\,\mathrm{mol\,L^{-1}}$ and $55.34\,\mathrm{mol\,L^{-1}}$, e.g., corresponds to a shift of U_{kin} by less than 2 mV. Even changing c_* by a factor of two would shift the kinetic reference voltage by less than 5 mV. The specific choice of $c_* = c^{\ominus}_{\mathrm{H_2O},\ell}$ has the advantage of making kinetic reference potentials of aqueous reactions independent of the number of solvating water molecules written in the reaction equation, as further discussed below.

With $c_* = c^{\ominus}_{\mathrm{H_2O},\ell} = 55.34\,\mathrm{mol\,L^{-1}}$, $c^{\ominus}_{\mathrm{H_2,aq}} = 0.771 \times 10^{-3}\,\mathrm{mol\,L^{-1}}$, and $c^{\ominus}_{\mathrm{O_2,aq}} = 1.252 \times$

$10^{-3}\,\mathrm{mol\,L^{-1}}$, Eq. (16) yields $U_{\mathrm{kin}} = 1.437\,\mathrm{V}$ for the water electrolysis reaction at $T = 25°\mathrm{C}$. In comparison to the standard equilibrium voltage $U_{\mathrm{eq}}^{\ominus} = 1.229\,\mathrm{V}$, this corresponds to an excess overvoltage of $\eta_{\mathrm{xs}} = U_{\mathrm{kin}} - U_{\mathrm{eq}}^{\ominus} = 0.208\,\mathrm{V}$ that quantifies the significant bias of the equilibrium voltage as a result of the concentration imbalance between the reactant and product state at standard conditions. To visualize the conceptual aspects, Figure 2(a) shows a schematic representation of the potential energy surface (PES) along a reaction coordinate. An arbitrary shape of the PES is shown. Also, the reaction coordinate should be regarded from a rather conceptual perspective to parametrize the entire pathway of electrolytic water splitting including both the oxygen evolution reaction (OER) and the hydrogen evolution reaction (HER), as well as their respective reaction intermediate states. We furthermore emphasize that the plotted energy curves refer to the *potential energy* of the system, including the electronic potential energy contribution that is controlled by the cell voltage. Unlike commonly used Gibbs free energy diagrams, the potential energy is *not* biased by unspecific contributions of the concentrations of reactants, products, and intermediates. The solid blue curve in Figure 2(a) shows the PES at U_{kin} where the reactant and product states are aligned and the reaction kinetics are determined by the specific shape of the potential energy barrier in between. As discussed above, U_{kin} can be interpreted as the equilibrium voltage for balanced concentrations between the reactant and product side, defined by the condition $\left(c_{\mathrm{H_2O},\ell}\right)^2 (c_*) = \left(c_{\mathrm{H_2}}\right)^2 \left(c_{\mathrm{O_2}}\right)$. The corresponding Gibbs free energies of the reactant and product side are schematically indicated by the upper solid horizontal bars in Figure 2(a). In contrast, at standard conditions, the concentration products are extremely unbalanced, $\left(c_{\mathrm{H_2O},\ell}^{\ominus}\right)^2 (c_*) \gg \left(c_{\mathrm{H_2,aq}}^{\ominus}\right)^2 \left(c_{\mathrm{O_2,aq}}^{\ominus}\right)$. The very small concentrations of H_2 and O_2 result in a significant lowering of the Gibbs free energy of the product side. Therefore, the potential energy contribution to the Gibbs free energy of the reactant side must be decreased accordingly with respect to the product side in order to maintain an overall equilibrium of the electrochemical reaction. This is achieved by decreasing the cell voltage from U_{kin} down to the standard equilibrium voltage $U_{\mathrm{eq}}^{\ominus}$, which produces a change in the PES as schematically shown by the dashed red curve in Figure 2(a). As a result, the water splitting reaction in the forward direction must overcome an additional potential energy corresponding to η_{xs}, which contributes to a suppression of the water splitting rate at cell voltages close to $U_{\mathrm{eq}}^{\ominus}$.

This rationale might be part of the reason why macroscopic water splitting rates have

not yet been achieved at cell voltages below $U \approx 1.4$–$1.5\,\mathrm{V}$ in low-temperature electrolysis[12]. A typical polarization curve of a proton-exchange membrane (PEM) water electrolyzer is shown in Fig. 2(b). The onset of observable electrolysis currents coincides well with the kinetic reference voltage $U_{\mathrm{kin}} = 1.437\,\mathrm{V}$. Accordingly, it would appear reasonable to redefine the activation overvoltage η_{act} to only represent the difference between the kinetic current curve and the kinetic reference voltage U_{kin}, whereas the excess overvoltage $\eta_{\mathrm{xs}} = U_{\mathrm{kin}} - U_{\mathrm{eq}}$ quantifies the contribution of the imbalance between the liquid water reactant concentration and the H_2 and O_2 product concentrations to the actual equilibrium voltage U_{eq}. To what extent the voltage range closer to $U_{\mathrm{eq}}^{\ominus} = 1.229\,\mathrm{V}$ could, in principle, be accessible in low-temperature electrolysis depends on the maximum reaction rates achievable at the kinetic reference voltage U_{kin} under ideal catalytic conditions. Ideal reaction rates will be estimated further below in the discussion of the OER. In the following, we will analyze both the HER and OER half-cell reactions individually.

C. Hydrogen evolution reaction (HER)

In acidic electrolyte, the HER and the reverse hydrogen oxidation reaction (HOR) proceed according to the equation

$$2\,\mathrm{H^+} \;+\; 2\,\mathrm{e^-} \;\rightleftharpoons\; \mathrm{H_2}\;, \tag{17}$$

and in alkaline conditions according to

$$2\,\mathrm{H_2O} \;+\; 2\,\mathrm{e^-} \;\rightleftharpoons\; \mathrm{H_2} \;+\; 2\,\mathrm{OH^-}\;. \tag{18}$$

Both reactions are coupled via the water autoprotolysis equilibrium

$$\mathrm{H_2O} \;\rightleftharpoons\; \mathrm{H^+} \;+\; \mathrm{OH^-}\;, \tag{19}$$

for which reason they have a common equilibrium potential $E_{\mathrm{eq}} = E_{\mathrm{RHE}}$ for given experimental conditions (RHE = reversible hydrogen electrode). However, the respective standard equilibrium potentials differ. Standard conditions define $c_{\mathrm{H^+}}^{\ominus} = 1\,\mathrm{mol\,L^{-1}}$ in the dilute limit for the acidic reaction (17), equivalent to a pH-value of 0. The corresponding standard equilibrium potential is the standard hydrogen electrode (SHE) potential $E_{\mathrm{eq}}^{\ominus,\mathrm{acid}} = E_{\mathrm{RHE}}^{\mathrm{pH}\,0} = E_{\mathrm{SHE}}$, which is commonly used as a fixed potential reference.

For the alkaline reaction (18), standard conditions define $c^{\ominus}_{\mathrm{OH^-}} = 1\,\mathrm{mol\,L^{-1}}$ in the dilute limit, equivalent to a pH-value of 14. The corresponding standard equilibrium potential is $E^{\ominus,\mathrm{alk}}_{\mathrm{eq}} = E^{\mathrm{pH}\,14}_{\mathrm{RHE}} = -0.828\,\mathrm{V_{SHE}}$, measured versus the standard equilibrium potential E_{SHE} of the acidic reaction.

According to Eq. (12), the kinetic reference potentials of the HER/HOR reactions (17) and (18) are given by

$$E^{\mathrm{acid}}_{\mathrm{kin}} = E^{\ominus,\mathrm{acid}}_{\mathrm{eq}} + \frac{RT}{2F}\,\ln\left(g^{\mathrm{acid}}_{\mathrm{r}}\right) + \frac{RT}{2F}\,\ln\left(\frac{\left(c^{\ominus}_{\mathrm{H_2,aq}}\right)\left(c_*\right)}{\left(c^{\ominus}_{\mathrm{H^+}}\right)^2}\right) + \frac{RT}{2F}\,\ln\left(\Gamma^{\mathrm{acid}}_{\mathrm{c,r}}\right)\ , \tag{20}$$

and

$$E^{\mathrm{alk}}_{\mathrm{kin}} = E^{\ominus,\mathrm{alk}}_{\mathrm{eq}} + \frac{RT}{2F}\,\ln\left(g^{\mathrm{alk}}_{\mathrm{r}}\right) + \frac{RT}{2F}\,\ln\left(\frac{\left(c^{\ominus}_{\mathrm{H_2,aq}}\right)\left(c^{\ominus}_{\mathrm{OH^-}}\right)^2}{\left(c^{\ominus}_{\mathrm{H_2O},\ell}\right)^2\left(c_*\right)}\right) + \frac{RT}{2F}\,\ln\left(\Gamma^{\mathrm{alk}}_{\mathrm{c,r}}\right)\ , \tag{21}$$

respectively. The combinatorial factors of the involved species are $g_{\mathrm{H_2O}} = 2$, $g_{\mathrm{H_2}} = 2$, $g_{\mathrm{H^+}} = 1$, and $g_{\mathrm{OH^-}} = 1$, so $g^{\mathrm{acid}}_{\mathrm{r}} = g_{\mathrm{H_2}}/g^2_{\mathrm{H^+}} = 2$ and $g^{\mathrm{alk}}_{\mathrm{r}} = g_{\mathrm{H_2}}\,g^2_{\mathrm{OH^-}}/g^2_{\mathrm{H_2O}} = 1/2$. As discussed above, it is reasonable to choose $c_* = c^{\ominus}_{\mathrm{H_2O},\ell} = 55.34\,\mathrm{mol\,L^{-1}}$. This particular choice brings the benefit that we could include additional water molecules at both sides of reaction (17) to describe the solvation of aqueous protons, e.g. in the form $\mathrm{H_3O^+}$, without changing the corresponding kinetic reference potential. As before, we neglect the insignificant contribution of $\Gamma^{\mathrm{acid}}_{\mathrm{c,r}}$ and $\Gamma^{\mathrm{alk}}_{\mathrm{c,r}}$. Together with $c^{\ominus}_{\mathrm{H_2,aq}} = 0.771 \times 10^{-3}\,\mathrm{mol\,L^{-1}}$, $c^{\ominus}_{\mathrm{H^+}} = 1\,\mathrm{mol\,L^{-1}}$, and $c^{\ominus}_{\mathrm{OH^-}} = 1\,\mathrm{mol\,L^{-1}}$, we obtain $E^{\mathrm{acid}}_{\mathrm{kin}} = -0.032\,\mathrm{V_{SHE}}$ and $E^{\mathrm{alk}}_{\mathrm{kin}} = -1.084\,\mathrm{V_{SHE}}$ from Eqs. (20) and (21), respectively, at $T = 25°\mathrm{C}$. Interestingly, even when expressed versus the corresponding RHE potentials $E^{\mathrm{pH}\,0}_{\mathrm{RHE}} = 0\,\mathrm{V_{SHE}}$ and $E^{\mathrm{pH}\,14}_{\mathrm{RHE}} = -0.828\,\mathrm{V_{SHE}}$, the kinetic reference potentials are markedly different in acidic and alkaline conditions with values $E^{\mathrm{acid}}_{\mathrm{kin}} = -0.032\ \mathrm{V}^{\mathrm{pH}\,0}_{\mathrm{RHE}}$ and $E^{\mathrm{alk}}_{\mathrm{kin}} = -0.256\ \mathrm{V}^{\mathrm{pH}\,14}_{\mathrm{RHE}}$, respectively.

It is well established that the HER/HOR reveal slower kinetics in alkaline electrolyte than in acid[14,15], but the origin of this effect is a matter of debate. Figure 3(a) shows the Tafel plots of experimentally determined kinetic currents. The data for acidic conditions was taken from published literature[13], where the HER kinetic currents had been measured in an acidic proton-exchange membrane (PEM) cell. For comparison, we measured the HER kinetic currents in an alkaline 1 M NaOH electrolyte using a three-electrode setup. Further experimental details are given in the caption of Figure 3. The electrode potentials are plotted versus the respective RHE for the given acidic and alkaline conditions and the corresponding

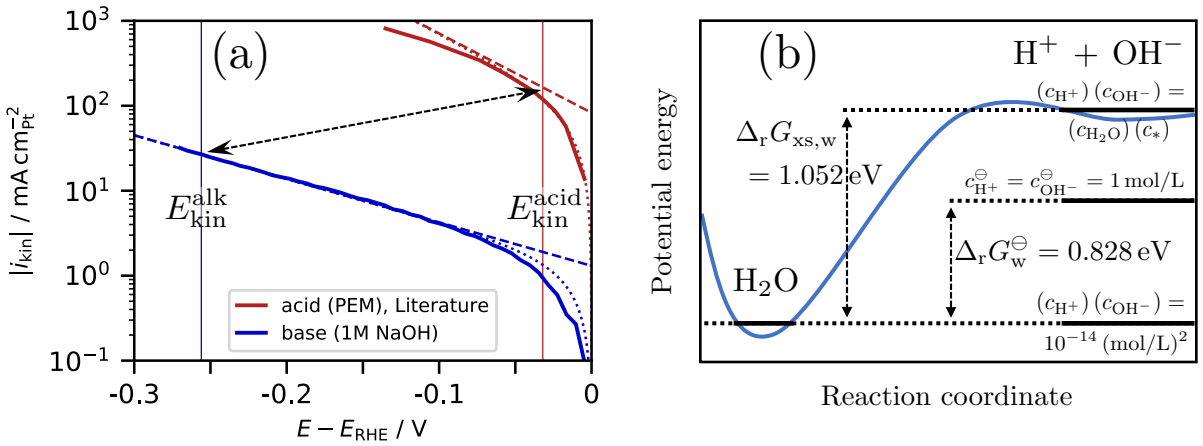

FIG. 3. (a) Experimental kinetic currents of the HER in acidic and alkaline electrolyte normalized to the surface area of the Pt catalyst. The data for acidic conditions was taken from published literature[13], where measurements had been performed in a proton-exchange membrane (PEM) cell at $p_{H_2} = 1$ bar and $T = 30°C$ using a Pt/C catalyst. Our measurements in alkaline conditions were performed in 1 M NaOH, saturated at $p_{H_2} = 1$ bar, using a three-electrode setup with a water-jacketed PTFE cell at $T = 30°C$. The Pt_{poly}-disk working electrode was rotated at 1600 rpm. Potentials were IR-corrected with an Ohmic resistance determined by impedance spectroscopy. Note that electrode potentials are shown versus the respective RHE for the given acidic and alkaline conditions. The positions of the corresponding kinetic reference potentials are indicated by vertical lines, assuming pH = 0 and pH = 14 for the acidic and alkaline experiments, respectively. To separate the HER and HOR contributions, we fitted the Butler-Volmer equation (1) to the experimental data in a potential range closely around the respective E_{kin}. Dotted curves show the fitted combined kinetic current of HER and HOR, dashed curves correspond to the fitted HER branch only. (b) Schematic representation of the potential energy along the reaction coordinate for water autoprotolysis. The corresponding Gibbs free energies of the reactant and product states are indicated by solid horizontal bars for balanced concentration conditions (top), for standard conditions (middle), and for equilibrium conditions (bottom).

kinetic reference potentials are indicated by vertical lines. The difference between the kinetic reference potentials at the RHE-scale demonstrates that the RHE equilibrium potential is more strongly biased by concentration imbalance in alkaline than in acidic conditions. Whereas the HER/HOR exchange current densities at $E^{pH\,0}_{RHE}$ and $E^{pH\,14}_{RHE}$ differ[15] by a factor

of the order of 100, the HER kinetic current at $E_{\mathrm{kin}}^{\mathrm{acid}}$ in acidic conditions is only about 6-times larger than the HER kinetic current at $E_{\mathrm{kin}}^{\mathrm{alk}}$ in alkaline conditions, indicated by the dashed arrow in Figure 3(a). Part of the apparent pH-effect in HER/HOR kinetics, when compared at the RHE potentials at pH = 0 and pH = 14, could therefore result from the fact that these RHE potentials are biased to different degrees by concentration imbalance.

But also when compared at the kinetic reference potentials, we still observe significant differences between the HER in acid versus base. Various mechanisms through which the pH-value can influence the kinetics of HER/HOR have been proposed, such as a change in adsorption energies of HER intermediates at the electrocatalyst surface[15,16], entropic barriers for proton transfer at the electrode–electrolyte interface[17,18], or interfacial water reorganisation[19]. The conclusion from our analysis that the unspecific concentration bias could, at least partially, contribute to the pH-effect is in agreement with the rather universal behavior observed for Pt/C, Ir/C, and Pd/C catalysts[15]. We discuss in the following that the ideal gas reference framework, upon which our present analysis is based, furthermore provides support for the hypothesis that water protolysis, or dissociation, is a limiting factor for the HER in alkaline conditions[14,20,21].

Water autoprotolysis. The water autoprotolysis reaction (19) plays a key role for an understanding of the differences of HER/HOR electrocatalysis in acidic versus alkaline conditions. The equilibrium constant of water autoprotolysis is $K_{\mathrm{w}} = (a_{\mathrm{H^+}})\,(a_{\mathrm{OH^-}}) = 1.0 \times 10^{-14}$, corresponding to a standard Gibbs free energy of reaction $\Delta_{\mathrm{r}}G_{\mathrm{w}}^{\ominus} = -k_{\mathrm{B}}T \ln K_{\mathrm{w}} = 0.828\,\mathrm{eV}$. However, standard conditions define unbalanced concentrations for the reactant and product side of reaction (19), with $c_{\mathrm{H_2O},\ell}^{\ominus} = 55.34\,\mathrm{mol\,L^{-1}}$ versus $c_{\mathrm{H^+}}^{\ominus} = c_{\mathrm{OH^-}}^{\ominus} = 1\,\mathrm{mol\,L^{-1}}$. Based on Eq. (7), we compute the unbiased excess Gibbs free energy of reaction of water autoprotolysis and obtain $\Delta_{\mathrm{r}}G_{\mathrm{xs,w}} = 1.052\,\mathrm{eV}$, where we used $c_* = c_{\mathrm{H_2O},\ell}^{\ominus} = 55.34\,\mathrm{mol\,L^{-1}}$ and $g_{\mathrm{r,w}} = 2$, and we neglected the quotient of activity coefficients. We realize that the value of the excess Gibbs free energy of water autoprotolysis $\Delta_{\mathrm{r}}G_{\mathrm{xs,w}} = 1.052\,\mathrm{eV}$ precisely corresponds to the absolute difference between the kinetic reference potentials of the HER/HOR in acid and base, $E_{\mathrm{kin}}^{\mathrm{alk}} - E_{\mathrm{kin}}^{\mathrm{acid}} = -1.052\,\mathrm{V}$, whereas the standard Gibbs free energy of water autoprotolysis $\Delta_{\mathrm{r}}G_{\mathrm{w}}^{\ominus} = 0.828\,\mathrm{eV}$ determines the shift of the standard equilibrium potentials, $E_{\mathrm{eq}}^{\ominus,\mathrm{alk}} - E_{\mathrm{eq}}^{\ominus,\mathrm{acid}} = E_{\mathrm{RHE}}^{\mathrm{pH\,14}} - E_{\mathrm{RHE}}^{\mathrm{pH\,0}} = -0.828\,\mathrm{V}$. We thus trace the relative shift of $-0.224\,\mathrm{V}$ between the kinetic reference potential in acid, $E_{\mathrm{kin}}^{\mathrm{acid}} = -0.032\ \mathrm{V}_{\mathrm{RHE}}^{\mathrm{pH\,0}}$, and base, $E_{\mathrm{kin}}^{\mathrm{alk}} = -0.256\ \mathrm{V}_{\mathrm{RHE}}^{\mathrm{pH\,14}}$, at the RHE-scale back to the difference between the excess and

standard Gibbs free energy of water autoprotolysis, $\Delta_r G_{xs,w} - \Delta_r G^{\ominus}_{w} = 0.224\,\mathrm{eV}$.

Figure 3(b) presents a schematic potential energy curve for water autoprotolysis. The reaction coordinate is essentially the distance between the dissociating H^+ and OH^-. In addition, the Gibbs free energies of the reactant and product states are schematically indicated by solid horizontal bars for different conditions. As discussed earlier, $\Delta_r G_{xs,w} = 1.052\,\mathrm{eV}$ corresponds to balanced concentration conditions, $(c_{H^+})\,(c_{OH^-}) = (c_{H_2O})\,(c_*)$, and it represents the intrinsic contribution of the potential energy surface to the Gibbs free energy difference between the dissociated product state of H^+ and OH^- and the H_2O reactant state. In contrast, $\Delta_r G^{\ominus}_{w}$ is reduced by the concentration imbalance between reactants and products due to the particular choice of the standard concentration of $c^{\ominus}_{H^+} = c^{\ominus}_{OH^-} = 1\,\mathrm{mol/L}$. Finally, at the actual equilibrium condition $(c_{H^+})\,(c_{OH^-}) = 10^{-14}\,(\mathrm{mol/L})^2$, the Gibbs free energy of the product state is equal to the one of the reactant state. In comparison to the acidic HER/HOR, the alkaline reaction (18) additionally involves water dissociation. Our analysis suggests that the $-0.828\,\mathrm{V}$-shift in the equilibrium RHE potential from $E^{\mathrm{pH}\,0}_{\mathrm{RHE}}$ to $E^{\mathrm{pH}\,14}_{\mathrm{RHE}}$ is not sufficient to fully compensate for the additional potential energy contribution required for water dissociation. This could, at least partially, be responsible for the slower kinetics of the HER/HOR in alkaline electrolyte. Our conclusion is in agreement with previous works[14,20,21] who identified water dissociation as the rate-determining step in alkaline conditions.

This hypothesis, however, had been questioned with the argument that the water dissociation reaction (19) is extremely fast[15,17], and therefore could not be rate limiting. Whereas this is true for the hydronium–hydroxide recombination, *i.e.* direction right to left, it is not true for the water protolysis, *i.e.* direction left to right. A simple estimation demonstrates this point, assuming that all protons generated from water autoprotolysis within a distance of 1 nm from the electrocatalyst surface would be available for HER. The rate constant of the hydronium–hydroxide recombination reaction was reported[22] with a value $k_{rec} = 1.3 \times 10^{11}\,\mathrm{s^{-1}(mol\,L^{-1})^{-1}}$, yielding a total recombination rate of $R_{rec} = c_{H^+}\,c_{OH^-}\,k_{rec} = 1.3 \times 10^{-3}\,\mathrm{mol\,L^{-1}s^{-1}}$, which, at equilibrium, is equal to the total water dissociation rate, $R_{diss} = R_{rec}$. Within the 1 nm-thick surface layer, it corresponds to $1.3 \times 10^{-13}\,\mathrm{mol\,cm^{-2}s^{-1}}$ water dissociation events, each of which contributing one proton. These would sustain an HER current density of $12.5 \times 10^{-9}\,\mathrm{A\,cm^{-2}}$, which is negligibly small. Thus, the water protolysis step is a limiting factor for the HER in alkaline conditions, and

feasible HER rates require an enhancement of water protolysis by the presence of a catalyst surface and the electrostatic fields within the electrochemical double-layer.

D. Oxygen evolution reaction (OER)

We now extend our analysis of kinetic reference potentials to the OER half-cell reaction. In acidic electrolyte, the OER, and the reverse oxygen reduction reaction (ORR), proceed according to the equation

$$2\,H_2O \;\rightleftharpoons\; O_2 \;+\; 4\,H^+ \;+\; 4\,e^- \;, \tag{22}$$

and in alkaline conditions according to

$$4\,OH^- \;\rightleftharpoons\; O_2 \;+\; 2\,H_2O \;+\; 4\,e^- \;. \tag{23}$$

Both reactions have a common equilibrium potential $E_{\mathrm{eq}} = 1.229\,\mathrm{V_{RHE}}$ versus the RHE potential for given experimental conditions. The standard equilibrium potentials are $E_{\mathrm{eq}}^{\ominus,\mathrm{acid}} = 1.229\,\mathrm{V_{SHE}}$ for the acidic reaction (22) and $E_{\mathrm{eq}}^{\ominus,\mathrm{alk}} = 0.401\,\mathrm{V_{SHE}}$ for the alkaline reaction (23), both given versus the fixed SHE potential. According to Eq. (12), the kinetic reference potentials of reactions (22) and (23) are given by

$$E_{\mathrm{kin}}^{\mathrm{acid}} \;=\; E_{\mathrm{eq}}^{\ominus,\mathrm{acid}} + \frac{RT}{4F}\,\ln\left(g_{\mathrm{r}}^{\mathrm{acid}}\right) + \frac{RT}{4F}\,\ln\left(\frac{\left(c_{\mathrm{H_2O},\ell}^{\ominus}\right)^2 (c_*)^3}{\left(c_{\mathrm{O_2,aq}}^{\ominus}\right)\left(c_{\mathrm{H^+}}^{\ominus}\right)^4}\right) + \frac{RT}{4F}\,\ln\left(\Gamma_{\mathrm{c,r}}^{\mathrm{acid}}\right) \;, \tag{24}$$

and

$$E_{\mathrm{kin}}^{\mathrm{alk}} \;=\; E_{\mathrm{eq}}^{\ominus,\mathrm{alk}} + \frac{RT}{4F}\,\ln\left(g_{\mathrm{r}}^{\mathrm{alk}}\right) + \frac{RT}{4F}\,\ln\left(\frac{\left(c_{\mathrm{OH^-}}^{\ominus}\right)^4}{\left(c_{\mathrm{O_2,aq}}^{\ominus}\right)\left(c_{\mathrm{H_2O},\ell}^{\ominus}\right)^2 (c_*)}\right) + \frac{RT}{4F}\,\ln\left(\Gamma_{\mathrm{c,r}}^{\mathrm{alk}}\right) \;, \tag{25}$$

respectively. The combinatorial factors of the involved species are $g_{\mathrm{H_2O}} = 2$, $g_{\mathrm{O_2}} = 2$, $g_{\mathrm{H^+}} = 1$, and $g_{\mathrm{OH^-}} = 1$, so $g_{\mathrm{r}}^{\mathrm{acid}} = g_{\mathrm{H_2O}}^2/(g_{\mathrm{O_2}}\, g_{\mathrm{H^+}}^4) = 2$ and $g_{\mathrm{r}}^{\mathrm{alk}} = g_{\mathrm{OH^-}}^4/(g_{\mathrm{O_2}}\, g_{\mathrm{H_2O}}^2) = 1/8$. As before, we choose $c_* = c_{\mathrm{H_2O},\ell}^{\ominus} = 55.34\,\mathrm{mol\,L^{-1}}$, and we neglect the insignificant contribution of $\Gamma_{\mathrm{c,r}}^{\mathrm{acid}}$ and $\Gamma_{\mathrm{c,r}}^{\mathrm{alk}}$. Together with $c_{\mathrm{O_2,aq}}^{\ominus} = 1.252 \times 10^{-3}\,\mathrm{mol\,L^{-1}}$ and $c_{\mathrm{H^+}}^{\ominus} = c_{\mathrm{OH^-}}^{\ominus} = 1\,\mathrm{mol\,L^{-1}}$, we obtain $E_{\mathrm{kin}}^{\mathrm{acid}} = 1.405\,\mathrm{V_{SHE}}$ and $E_{\mathrm{kin}}^{\mathrm{alk}} = 0.353\,\mathrm{V_{SHE}}$ from Eqs. (24) and (25), respectively, at $T = 25°\mathrm{C}$, given versus the fixed SHE reference. Measured with respect to the corresponding RHE potentials, the acidic and alkaline kinetic reference potentials are $E_{\mathrm{kin}}^{\mathrm{acid}} = 1.405\,\mathrm{V_{RHE}^{pH\,0}}$ and $E_{\mathrm{kin}}^{\mathrm{alk}} = 1.181\,\mathrm{V_{RHE}^{pH\,14}}$. We note that the difference between the kinetic reference potentials

of the OER and HER is precisely equal to the kinetic reference voltage $U_{\mathrm{kin}} = 1.437\,\mathrm{V}$ of the overall water electrolysis reaction in both acidic and alkaline conditions, which supports the consistency of our results.

Importantly, the kinetic reference potentials of the acidic and alkaline OER are different at the corresponding RHE scales. It is interesting to note that the value of $E_{\mathrm{kin}}^{\mathrm{acid}} = 1.405\,\mathrm{V}_{\mathrm{RHE}}^{\mathrm{pH\,0}}$ agrees well with experimentally observed OER onset potentials in acid around 1.4–$1.5\,\mathrm{V}_{\mathrm{RHE}}^{\mathrm{pH\,0}}$ for RuO_2 and IrO_2 catalysts[23–26]. Could it thus be that these catalysts are already close to optimal, excluding the existence of the "philosophers' stone" catalyst that would enable OER onset close to $E_{\mathrm{eq}}^{\ominus,\mathrm{acid}} = 1.229\,\mathrm{V}_{\mathrm{RHE}}^{\mathrm{pH\,0}}$? Whereas we do not claim to give a conclusive answer to this question, we wish to contribute a novel perspective. As discussed in Part I. of the present series[8], the ideal association/dissociation kinetics of the ideal gas framework could be regarded as an upper bound for real association/dissociation rates. At $E_{\mathrm{kin}}^{\mathrm{acid}} = 1.405\,\mathrm{V}_{\mathrm{RHE}}^{\mathrm{pH\,0}}$ the OER reactant and product states are aligned within the overall potential energy landscape of the system in an acidic environment. An ideal OER catalyst would then provide a reaction pathway along which the potential energy profile is entirely flat. In such ideal scenario at the kinetic reference potential, the renormalized rate constant of reaction (22) would be close to the ideal rate constant k_{id}, as discussed in Part I. of this series, for which we estimated $k_{\mathrm{id}} \approx 10^{12}$–$10^{13}\,\mathrm{s}^{-1}$ at room temperature. Note that k_{id} is an effective first-order rate constant that also describes higher-order reactions after appropriate renormalization, as discussed in detail in Part I. For the case of surface reactions, it can be interpreted as an ideal turnover frequency (TOF) per surface site. The maximum area-specific reaction rate is then given by $r_{\mathrm{max}} = (N_{\mathrm{s}}/\mathcal{A})\,k_{\mathrm{id}}$, where $N_{\mathrm{s}}/\mathcal{A}$ is the number of catalytically active sites per surface area. The latter is typically of the order of $N_{\mathrm{s}}/\mathcal{A} \approx 10^{-1}\,\mathrm{Å}^{-2}$, yielding $r_{\mathrm{max}} \approx 10^{27}$–$10^{28}\,\mathrm{cm}^{-2}\,\mathrm{s}^{-1} \approx 10^{4}\,\mathrm{mol}\,\mathrm{cm}^{-2}\,\mathrm{s}^{-1}$. This corresponds to a maximum kinetic current density of the order of $i_{\mathrm{kin,max}} = r_{\mathrm{max}}F \approx 10^{9}\,\mathrm{A}\,\mathrm{cm}^{-2}$ at the kinetic reference potential E_{kin} on an ideal electrocatalyst.

At a real electrocatalyst surface in a real electrolyte, many "non-ideal" factors contribute to a reduction of the actual kinetic current density compared to the ideal one. All of these factors essentially originate from the specific shape of the system's potential energy surface. If, e.g., a potential energy barrier of height ΔE_{act} separates the reactant and product state of the rate-determining step, the respective rate constant is scaled down by a factor $\exp(-\Delta E_{\mathrm{act}}/k_{\mathrm{B}}T)$. To achieve macroscopic current densities of the order of $1\,\mathrm{A}\,\mathrm{cm}^{-2}$

at $E_{\mathrm{kin}}^{\mathrm{acid}} = 1.405\,\mathrm{V}_{\mathrm{RHE}}^{\mathrm{pH\,0}}$, the maximum allowed potential energy barrier would thus be of the order of $\Delta E_{\mathrm{act}} \approx 0.5\,\mathrm{eV}$, computed based on the value of $i_{\mathrm{kin,max}}$ estimated above. At an electrode potential equal to $E_{\mathrm{eq}}^{\ominus,\mathrm{acid}} = 1.229\,\mathrm{V}_{\mathrm{RHE}}^{\mathrm{pH\,0}}$, the product state of the OER (22) is raised by $(-e)(E_{\mathrm{eq}}^{\ominus,\mathrm{acid}} - E_{\mathrm{kin}}^{\mathrm{acid}}) = e\,\eta_{\mathrm{xs}}^{\mathrm{acid}} = 0.176\,\mathrm{eV}$ *per electron* with respect to the reactant state. A certain fraction $\alpha e\,\eta_{\mathrm{xs}}^{\mathrm{acid}}$ would add to the height of the potential energy barrier of the rate-determining step, which would have to be compensated by further catalyst improvements in order to shift the OER onset closer to $E_{\mathrm{eq}}^{\ominus,\mathrm{acid}}$. Although this is only a rough order-of-magnitude estimate, it shows how the kinetic reference potential provides a point of orientation for the question at which potential an optimal electrocatalyst would provide macroscopic kinetic currents for a given reaction. Whereas our analysis does not exclude the existence of the "philosophers' stone" catalyst for the OER in acidic conditions, the respective criteria to be met in terms of potential energy barriers are rather tight. In alkaline conditions, however, an entirely different situation is found. The kinetic reference potential $E_{\mathrm{kin}}^{\mathrm{alk}} = 1.181\,\mathrm{V}_{\mathrm{RHE}}^{\mathrm{pH\,14}}$ is shifted slightly negative with respect to the equilibrium potential $E_{\mathrm{eq}}^{\ominus,\mathrm{alk}} = 1.229\,\mathrm{V}_{\mathrm{RHE}}^{\mathrm{pH\,14}}$. Thus, based on the present analysis, there appears to be significantly more room for improvement of OER electrocatalyst materials in alkaline rather than acidic conditions.

E. Lattice oxygen evolution reaction (LOER)

Equally important as the activity of an electrocatalyst material towards a target reaction is its stability, so the suppression of unwanted degradation reactions. This aspect is particularly important in OER electrocatalysis, because it has been experimentally shown[23,27,28] and theoretically proven[29] that there exists an intimate correlation between activity and corrosion of metal oxide OER catalysts. This was explained by the thermodynamic destabilization of the lattice oxygen anion under OER conditions, resulting in what was termed the lattice oxygen evolution reaction (LOER)[29]. Consequently, the LOER has gained significant attention in OER electrocatalysis research in recent years[30]. Although the OER and LOER are thermodynamically coupled, examples exist where no significant corrosion of metal oxide catalysts was observed during OER. Crystalline IrO_2 films, e.g., have demonstrated remarkable stability under OER conditions[31]. Such decoupling of OER and LOER might be explained by kinetic limitations of the LOER process[29–31].

LOER of IrO_2. In the following, we apply the concept of kinetic reference potentials to a prominent example of an LOER process for IrO_2. The thermodynamic driving force for the LOER is the oxidation of the lattice oxygen anion towards O_2. The remaining metal cation can undergo dissolution in different oxidation states. For the case of IrO_2, with a formal Ir(IV)-valency, it is unlikely that the iridium cation gets dissolved with an unchanged valency, because a stable aqueous Ir^{4+}_{aq} is not known to the best of our knowledge. In contrast, aqueous Ir^{3+}_{aq} is well-known to be particularly stable[32], for which reason electrochemical iridium dissolution has been associated with this species[33]. We therefore consider the LOER process

$$IrO_2 \rightleftharpoons Ir^{3+}_{aq} + O_2 + 3\,e^- \,. \tag{26}$$

It is particularly noteworthy that this LOER involves the *reduction* of the iridium cation, although the overall process is an oxidation reaction. The thermodynamic driving force for the oxidation of the lattice oxygen anion can thus trigger an increased dissolution of the metal cation in a reduced state with increasing electrode potential, a phenomenon which might appear paradoxical at first glance. Similar corrosion processes are known from cathode materials for Li-ion batteries[34].

We first compute the standard equilibrium potential of the LOER reaction (26) in acidic electrolyte. For this, we note that, formally, it can be written as a sequence of a reductive iridium dissolution (diss) step, $IrO_2 + 4\,H^+ + e^- \rightleftharpoons Ir^{3+}_{aq} + 2\,H_2O$, and a subsequent OER, $2\,H_2O \rightleftharpoons O_2 + 4\,H^+ + 4\,e^-$, with standard equilibrium potentials[35] $E^{\ominus}_{\mathrm{eq,diss}} = 0.233\,V_{SHE}$ and $E^{\ominus}_{\mathrm{eq,OER}} = 1.229\,V_{SHE}$, respectively. The standard equilibrium potential of the LOER (26) is thus obtained from the equality $(-3e)(E - E^{\ominus}_{\mathrm{eq,LOER}}) = (-4e)(E - E^{\ominus}_{\mathrm{eq,OER}}) + e(E - E^{\ominus}_{\mathrm{eq,diss}})$, yielding $E^{\ominus}_{\mathrm{eq,LOER}} = \frac{1}{3}(4\,E^{\ominus}_{\mathrm{eq,OER}} - E^{\ominus}_{\mathrm{eq,diss}}) = 1.561\,V_{SHE}$. According to Eq. (12), the kinetic reference potential of the LOER (26) is then given by

$$E_{\mathrm{kin,LOER}} = E^{\ominus}_{\mathrm{eq,LOER}} + \frac{RT}{3F}\,\ln(g_r) + \frac{RT}{3F}\,\ln\left(\frac{\left(c^{\ominus}_{IrO_2}\right)(c_*)}{\left(c^{\ominus}_{Ir^{3+}_{aq}}\right)\left(c^{\ominus}_{O_2,aq}\right)}\right) + \frac{RT}{3F}\,\ln(\Gamma_{c,r}) \,. \tag{27}$$

The combinatorial factors of the involved species are $g_{IrO_2} = 2$, $g_{O_2} = 2$, and $g_{Ir^{3+}_{aq}} = 1$, so $g_r = g_{IrO_2}/(g_{O_2}\,g_{Ir^{3+}_{aq}}) = 1$. As before, we choose $c_* = c^{\ominus}_{H_2O,\ell} = 55.34\,mol\,L^{-1}$, and we neglect the insignificant contribution of $\Gamma_{c,r}$. The standard concentration of the dissolved Ir^{3+}_{aq} is $c^{\ominus}_{Ir^{3+}_{aq}} = 1\,mol\,L^{-1}$, and $c^{\ominus}_{O_2,aq} = 1.252 \times 10^{-3}\,mol\,L^{-1}$ at the standard pressure of

$p^{\ominus} = 1\,\mathrm{bar}$. The standard-state concentration of IrO_2 units in the rutile IrO_2 crystal is $c^{\ominus}_{IrO_2} = 51.81\,\mathrm{mol\,L^{-1}}$, computed from the corresponding lattice constants[36]. A comment on this unusual notion of a "concentration of formula units" in a crystal is given below. With these values, we obtain $E_{\mathrm{kin,LOER}} = 1.686\,\mathrm{V_{SHE}}$ at $T = 25°\mathrm{C}$. Consequently, there exists a potential window in between the kinetic reference potential $E_{\mathrm{kin,OER}} = 1.405\,\mathrm{V_{SHE}}$ of the desired OER and $E_{\mathrm{kin,LOER}} = 1.686\,\mathrm{V_{SHE}}$ of the undesired LOER for IrO_2. Our analysis suggests that within this potential range significant OER rates are possible, while LOER-related corrosion of IrO_2 could be kinetically suppressed. At $E_{\mathrm{kin,LOER}}$ the contribution of the system's potential energy landscape to the Gibbs free energy of the LOER reactant and product states is balanced. In the potential range below $E_{\mathrm{kin,LOER}}$, the Gibbs free energy along the LOER pathway necessarily contains uphill potential energy contributions, enabling kinetic stabilization of the IrO_2 catalyst. Of course, kinetic suppression of LOER can further extend to the potential range beyond $E_{\mathrm{kin,LOER}}$ if a sufficiently high potential energy barrier separates the reactants from products.

The notion of a "concentration of formula units" in a crystal requires some clarification. For the case of crystalline solids, we clearly reach a limit where the distinction between individual entities becomes ambiguous. In principle, the entire IrO_2 crystal could be regarded as one molecular entity. However, in the present example, the LOER involves individual units of the crystal with iridium cations getting dissolved one by one. We therefore treat each IrO_2 unit as an individual molecular entity, with a corresponding concentration $c^{\ominus}_{IrO_2}$. We furthermore note that we used "bulk" quantities of crystalline IrO_2 to compute the kinetic reference potential. However, the LOER occurs at the electrode–electrolyte boundary, where the stability of IrO_2 units is generally decreased compared to the bulk due to the defects introduced and represented by the interface. Therefore, the computed "bulk" kinetic reference potential rather represents an upper bound for kinetic reference potentials that include the surface/interface energetics. We therefore emphasize that the morphology of the electrode–electrolyte boundary has an influence on the LOER kinetics. Finally, the presently considered LOER (26) is only one possibility of an LOER for IrO_2. Other LOER processes involving dissolved iridium species with different oxidation states could further limit the kinetic stability range. Nevertheless, reaction (26) is a feasible example of an LOER, and our analysis shows how the concept of kinetic reference potentials could be useful to distinguish thermodynamic from kinetic aspects in the study of electrocatalyst stability.

LOER of CoOOH. A similar coupling of lattice oxygen evolution and metal cation reduction and dissolution can occur for CoOOH, a prominent OER catalyst in alkaline conditions[37,38]. Since both aqueous Co^{3+}_{aq} and Co^{2+}_{aq} are known, we consider the two LOER processes in alkaline conditions

$$CoOOH \; + \; OH^- \; \rightleftharpoons \; Co^{3+}_{aq} \; + \; O_2 \; + \; H_2O \; + \; 4\,e^- \tag{28}$$

and

$$CoOOH \; + \; OH^- \; \rightleftharpoons \; Co^{2+}_{aq} \; + \; O_2 \; + \; H_2O \; + \; 3\,e^- \; . \tag{29}$$

Whereas in the first process the cobalt cation gets dissolved with an unchanged valency, the second process involves the dissolution of the cobalt cation with a reduced valency, similar to the LOER of IrO_2 considered above. Nevertheless, also the second LOER is an overall oxidation reaction. To compute the standard equilibrium potentials of reactions (28) and (29) at pH = 14, we first formally compute the standard equilibrium potentials of the acidic counterparts at pH = 0. For this purpose, we first add an H^+ at both sides of the reaction, and then use the standard Gibbs free energies of formation[39] $\Delta G^{\ominus}_{f,CoOOH} = -4.002\,eV$, $\Delta G^{\ominus}_{f,Co^{3+}_{aq}} = 1.385\,eV$, and $\Delta G^{\ominus}_{f,Co^{2+}_{aq}} = -0.576\,eV$, noting that the $\Delta G^{\ominus}_f$ of O_2 and H^+ are zero by definition. We thus obtain $E^{\ominus,pH\,0}_{eq,LOER,I} = 1.347\,V_{SHE}$ and $E^{\ominus,pH\,0}_{eq,LOER,II} = 1.142\,V_{SHE}$ for the acidic counterparts of reactions (28) and (29), respectively, at $T = 25°C$. The corresponding alkaline standard equilibrium potentials at pH = 14 are then obtained from the Nernst equations $E^{\ominus,pH\,14}_{eq,LOER,I} = E^{\ominus,pH\,0}_{eq,LOER,I} - (RT/4F)\ln(10)\,pH = 1.140\,V_{SHE} = 1.968\,V^{pH\,14}_{RHE}$ and $E^{\ominus,pH\,14}_{eq,LOER,II} = E^{\ominus,pH\,0}_{eq,LOER,II} - (RT/3F)\ln(10)\,pH = 0.866\,V_{SHE} = 1.694\,V^{pH\,14}_{RHE}$. According to Eq. (12), the kinetic reference potentials of the LOER processes (28) and (29) are given by

$$E_{kin,LOER,I} \; = \; E^{\ominus,pH\,14}_{eq,LOER,I} + \frac{RT}{4F}\,\ln\left(g_{r,I}\right) + \frac{RT}{4F}\,\ln\left(\frac{\left(c^{\ominus}_{CoOOH}\right)\left(c^{\ominus}_{OH^-}\right)\left(c_*\right)}{\left(c^{\ominus}_{Co^{3+}_{aq}}\right)\left(c^{\ominus}_{O_2,aq}\right)\left(c^{\ominus}_{H_2O,\ell}\right)}\right) + \frac{RT}{4F}\,\ln\left(\Gamma_{c,r,I}\right) \tag{30}$$

and

$$E_{kin,LOER,II} \; = \; E^{\ominus,pH\,14}_{eq,LOER,II} + \frac{RT}{3F}\,\ln\left(g_{r,II}\right) + \frac{RT}{3F}\,\ln\left(\frac{\left(c^{\ominus}_{CoOOH}\right)\left(c^{\ominus}_{OH^-}\right)\left(c_*\right)}{\left(c^{\ominus}_{Co^{2+}_{aq}}\right)\left(c^{\ominus}_{O_2,aq}\right)\left(c^{\ominus}_{H_2O,\ell}\right)}\right) + \frac{RT}{3F}\,\ln\left(\Gamma_{c,r,II}\right) \; , \tag{31}$$

respectively. The combinatorial factors of the involved species are $g_{\mathrm{CoOOH}} = g_{\mathrm{O_2}} = g_{\mathrm{H_2O}} = 2$, and $g_{\mathrm{Co^{3+}_{aq}}} = g_{\mathrm{Co^{2+}_{aq}}} = g_{\mathrm{OH^-}} = 1$, so $g_{\mathrm{r,I}} = g_{\mathrm{r,II}} = 1/2$. As before, we choose $c_* = c^{\ominus}_{\mathrm{H_2O},\ell} = 55.34\,\mathrm{mol\,L^{-1}}$, and we neglect the insignificant contributions of $\Gamma_{\mathrm{c,r,I/II}}$. The standard concentration of the dissolved ions is $c^{\ominus}_{\mathrm{Co^{3+}_{aq}}} = c^{\ominus}_{\mathrm{Co^{2+}_{aq}}} = c^{\ominus}_{\mathrm{OH^-}} = 1\,\mathrm{mol\,L^{-1}}$, and $c^{\ominus}_{\mathrm{O_2,aq}} = 1.252 \times 10^{-3}\,\mathrm{mol\,L^{-1}}$ at the standard pressure of $p^{\ominus} = 1\,\mathrm{bar}$. The standard-state concentration of CoOOH units in the heterogenite β-CoOOH crystal is $c^{\ominus}_{\mathrm{CoOOH}} = 53.82\,\mathrm{mol\,L^{-1}}$, computed from the corresponding lattice constants[40]. With these values, we obtain $E_{\mathrm{kin,LOER,I}} = 2.032\,\mathrm{V^{pH\,14}_{RHE}}$ and $E_{\mathrm{kin,LOER,II}} = 1.780\,\mathrm{V^{pH\,14}_{RHE}}$ at $T = 25°\mathrm{C}$ for reactions (28) and (29), respectively. The kinetic reference potential of the LOER process (29) involving reductive cobalt dissolution is significantly lower, and this process would likely be limiting for the CoOOH catalyst stability during OER. Nevertheless, the corresponding value of $E_{\mathrm{kin,LOER,II}} = 1.780\,\mathrm{V^{pH\,14}_{RHE}}$ leaves a significant potential window where the CoOOH catalyst can be active towards OER whilst being kinetically stabilized against LOER, in agreement with the experimentally observed stability of CoOOH films during OER[38].

IV. CONCLUSIONS

The ideal gas reference for association/dissociation reactions developed in Part I. of the present series was extended to electrochemical reactions, leading to the definition of kinetic reference potentials and voltages for half-cell and full-cell reactions, respectively. The kinetic reference potential can be interpreted as the equilibrium potential for balanced concentrations between the reactant and product side, as defined by the ideal law of mass action. Furthermore, at the kinetic reference potential, the contributions of the system's potential energy landscape to the Gibbs free energy of reactants and products are equal, meaning that the reactant and product states are "aligned". For simple unimolecular electrochemical electron-transfer reactions, the kinetic reference potential coincides with the standard equilibrium potential. For electrolysis reactions involving reactants and products in different states of aggregation, the standard equilibrium potential is strongly biased by the imbalance between the reactant and product concentrations. In contrast, the kinetic reference potential represents an intrinsic reference point along the potential axis, independent of such bias. For water electrolysis, the kinetic reference voltage agrees remarkably well with experimentally observed onset voltages for macroscopic electrolysis rates. For the hydrogen evolution

half-cell reaction, we found differences between the kinetic reference potentials in acidic and alkaline electrolyte that could contribute to the pH-effect in HER/HOR kinetics. For the oxygen evolution half-cell reaction, our analysis suggests that there exists more room for improvement of OER electrocatalysis in alkaline rather than acidic conditions. Finally, we investigated the kinetic reference potentials for several LOER processes of IrO_2 and CoOOH electrocatalysts. For both catalysts, LOER could be facilitated by a concomitant reduction of the metal cation. The respective kinetic reference potentials for LOER were found to be more positive than the OER kinetic reference potential, defining a potential window where the electrocatalyst materials can combine OER activity with kinetic stability against LOER.

ACKNOWLEDGMENTS

T.B. acknowledges financial support in the form of a research fellowship grant funded by the SNSF (Swiss National Science Foundation). R.M. acknowledges financial support from the South African Department of Science and Innovation in the form of HySA/Catalysis Centre of Competence programme funding.

AUTHOR DECLARATIONS

The authors have no conflicts to disclose.

DATA AVAILABILITY STATEMENT

The data that support the findings of this study are available from the corresponding author upon reasonable request.

REFERENCES

[1]A. J. Bard and L. R. Faulkner, *Electrochemical Methods: Fundamentals and Applications*, 2nd ed. (John Wiley & Sons Ltd, New York, 2010).

[2]J. Newman and K. E. Thomas-Alyea, *Electrochemical Systems*, 3rd ed. (John Wiley & Sons, Inc., Hoboken, New Jersey, 2004).

[3]A. C. Garcia and M. T. M. Koper, "Effect of saturating the electrolyte with oxygen on the activity for the oxygen evolution reaction," ACS Catalysis **8**, 9359–9363 (2018).

[4]M. Suermann, T. J. Schmidt, and F. N. Büchi, "Cell performance determining parameters in high pressure water electrolysis," Electrochimica Acta **211**, 989 – 997 (2016).

[5]C. L. Young, ed., *IUPAC Solubility Data Series Volume 5/6, Hydrogen and Deuterium* (Pergamon Press, Oxford, 1981).

[6]R. Battino, ed., *IUPAC Solubility Data Series Volume 7, Oxygen and Ozone* (Pergamon Press, Oxford, 1981).

[7]S. A. Stern, F. Bagenal, K. Ennico, G. R. Gladstone, W. M. Grundy, W. B. McKinnon, J. M. Moore, C. B. Olkin, J. R. Spencer, H. A. Weaver, L. A. Young, T. Andert, J. Andrews, M. Banks, B. Bauer, J. Bauman, O. S. Barnouin, P. Bedini, K. Beisser, R. A. Beyer, S. Bhaskaran, R. P. Binzel, E. Birath, M. Bird, D. J. Bogan, A. Bowman, V. J. Bray, M. Brozovic, C. Bryan, M. R. Buckley, M. W. Buie, B. J. Buratti, S. S. Bushman, A. Calloway, B. Carcich, A. F. Cheng, S. Conard, C. A. Conrad, J. C. Cook, D. P. Cruikshank, O. S. Custodio, C. M. Dalle Ore, C. Deboy, Z. J. B. Dischner, P. Dumont, A. M. Earle, H. A. Elliott, J. Ercol, C. M. Ernst, T. Finley, S. H. Flanigan, G. Fountain, M. J. Freeze, T. Greathouse, J. L. Green, Y. Guo, M. Hahn, D. P. Hamilton, S. A. Hamilton, J. Hanley, A. Harch, H. M. Hart, C. B. Hersman, A. Hill, M. E. Hill, D. P. Hinson, M. E. Holdridge, M. Horanyi, A. D. Howard, C. J. A. Howett, C. Jackman, R. A. Jacobson, D. E. Jennings, J. A. Kammer, H. K. Kang, D. E. Kaufmann, P. Kollmann, S. M. Krimigis, D. Kusnierkiewicz, T. R. Lauer, J. E. Lee, K. L. Lindstrom, I. R. Linscott, C. M. Lisse, A. W. Lunsford, V. A. Mallder, N. Martin, D. J. McComas, R. L. McNutt, D. Mehoke, T. Mehoke, E. D. Melin, M. Mutchler, D. Nelson, F. Nimmo, J. I. Nunez, A. Ocampo, W. M. Owen, M. Paetzold, B. Page, A. H. Parker, J. W. Parker, F. Pelletier, J. Peterson, N. Pinkine, M. Piquette, S. B. Porter, S. Protopapa, J. Redfern, H. J. Reitsema, D. C. Reuter, J. H. Roberts, S. J. Robbins, G. Rogers, D. Rose, K. Runyon, K. D. Retherford, M. G. Ryschkewitsch, P. Schenk, E. Schindhelm, B. Sepan, M. R. Showalter, K. N. Singer, M. Soluri, D. Stanbridge, A. J. Steffl, D. F. Strobel, T. Stryk, M. E. Summers, J. R. Szalay, M. Tapley, A. Taylor, H. Taylor, H. B. Throop, C. C. C. Tsang, G. L. Tyler, O. M. Umurhan, A. J. Verbiscer, M. H. Versteeg, M. Vincent, R. Webbert, S. Weidner, G. E. Weigle, O. L. White, K. Whittenburg, B. G. Williams, K. Williams, S. Williams, W. W. Woods, A. M. Zangari, and E. Zirnstein, "The pluto system: Initial results from

its exploration by new horizons," Science **350** (2015), 10.1126/science.aad1815.

[8]T. Binninger, A. Heinritz, and R. Mohamed, "Ideal gas reference for association and dissociation reactions: I. Basic concepts," This Journal **?**, ? (?), submitted 2021.

[9]A. D. McNaught and A. Wilkinson, eds., *IUPAC. Compendium of Chemical Terminology, 2nd ed. (the "Gold Book")* (Blackwell Scientific Publications, Oxford, 1997) online version (2019-) created by S. J. Chalk.

[10]P. J. Linstrom and W. G. Mallard, eds., *NIST Chemistry WebBook, NIST Standard Reference Database Number 69* (National Institute of Standards and Technology, Gaithersburg MD, 20899, 2018) retrieved May 17, 2020.

[11]J. D. Cox, D. D. Wagman, and V. A. Medvedev, *CODATA Key Values for Thermodynamics* (Hemisphere Publishing Corp., New York, 1989).

[12]U. Babic, M. Suermann, F. N. Büchi, L. Gubler, and T. J. Schmidt, "Review—identifying critical gaps for polymer electrolyte water electrolysis development," Journal of The Electrochemical Society **164**, F387–F399 (2017).

[13]B. M. Stühmeier, M. R. Pietsch, J. N. Schwämmlein, and H. A. Gasteiger, "Pressure and temperature dependence of the hydrogen oxidation and evolution reaction kinetics on pt electrocatalysts via PEMFC-based hydrogen-pump measurements," Journal of The Electrochemical Society **168**, 064516 (2021).

[14]D. Strmcnik, M. Uchimura, C. Wang, R. Subbaraman, N. Danilovic, D. van der Vliet, A. P. Paulikas, V. R. Stamenkovic, and N. M. Markovic, "Improving the hydrogen oxidation reaction rate by promotion of hydroxyl adsorption," Nature Chem. **5**, 300–306 (2013).

[15]J. Durst, A. Siebel, C. Simon, F. Hasché, J. Herranz, and H. A. Gasteiger, "New insights into the electrochemical hydrogen oxidation and evolution reaction mechanism," Energy Environ. Sci. **7**, 2255–2260 (2014).

[16]W. Sheng, Z. Zhuang, M. Gao, J. Zheng, J. G. Chen, and Y. Yan, "Correlating hydrogen oxidation and evolution activity on platinum at different ph with measured hydrogen binding energy," Nat. Commun. **6**, 5848 (2015).

[17]J. Rossmeisl, K. Chan, E. Skúlason, M. E. Björketun, and V. Tripkovic, "On the ph dependence of electrochemical proton transfer barriers," Catalysis Today **262**, 36 – 40 (2016).

[18]A. R. Zeradjanin, G. Polymeros, C. Toparli, M. Ledendecker, N. Hodnik, A. Erbe, M. Rohwerder, and F. La Mantia, "What is the trigger for the hydrogen evolution reaction?

– towards electrocatalysis beyond the sabatier principle," Phys. Chem. Chem. Phys. **22**, 8768–8780 (2020).

[19]I. Ledezma-Yanez, W. D. Z. Wallace, P. Sebastián-Pascual, V. Climent, J. M. Feliu, and M. T. M. Koper, "Interfacial water reorganization as a ph-dependent descriptor of the hydrogen evolution rate on platinum electrodes," Nature Energy **2**, 17031 (2017).

[20]Y. Zheng, Y. Jiao, Y. Zhu, L. H. Li, Y. Han, Y. Chen, M. Jaroniec, and S.-Z. Qiao, "High electrocatalytic hydrogen evolution activity of an anomalous ruthenium catalyst," Journal of the American Chemical Society **138**, 16174–16181 (2016).

[21]C. Hu, L. Zhang, and J. Gong, "Recent progress made in the mechanism comprehension and design of electrocatalysts for alkaline water splitting," Energy Environ. Sci. **12**, 2620–2645 (2019).

[22]M. Eigen and L. De Maeyer, "Untersuchungen über die kinetik der neutralisation. i," Zeitschrift für Elektrochemie, Berichte der Bunsengesellschaft für physikalische Chemie **59**, 986–993 (1955).

[23]N. Danilovic, R. Subbaraman, K.-C. Chang, S. H. Chang, Y. J. Kang, J. Snyder, A. P. Paulikas, D. Strmcnik, Y.-T. Kim, D. Myers, V. R. Stamenkovic, and N. M. Markovic, "Activity–stability trends for the oxygen evolution reaction on monometallic oxides in acidic environments," The Journal of Physical Chemistry Letters **5**, 2474–2478 (2014).

[24]D. F. Abbott, D. Lebedev, K. Waltar, M. Povia, M. Nachtegaal, E. Fabbri, C. Copéret, and T. J. Schmidt, "Iridium oxide for the oxygen evolution reaction: Correlation between particle size, morphology, and the surface hydroxo layer from operando xas," Chemistry of Materials **28**, 6591–6604 (2016).

[25]R. R. Rao, M. J. Kolb, N. B. Halck, A. F. Pedersen, A. Mehta, H. You, K. A. Stoerzinger, Z. Feng, H. A. Hansen, H. Zhou, L. Giordano, J. Rossmeisl, T. Vegge, I. Chorkendorff, I. E. L. Stephens, and Y. Shao-Horn, "Towards identifying the active sites on RuO_2(110) in catalyzing oxygen evolution," Energy Environ. Sci. **10**, 2626–2637 (2017).

[26]A. Hartig-Weiss, M. Miller, H. Beyer, A. Schmitt, A. Siebel, A. T. S. Freiberg, H. A. Gasteiger, and H. A. El-Sayed, "Iridium oxide catalyst supported on antimony-doped tin oxide for high oxygen evolution reaction activity in acidic media," ACS Applied Nano Materials **3**, 2185–2196 (2020).

[27]K. J. May, C. E. Carlton, K. A. Stoerzinger, M. Risch, J. Suntivich, Y.-L. Lee, A. Grimaud, and Y. Shao-Horn, "Influence of oxygen evolution during water oxidation on the surface

of perovskite oxide catalysts," The Journal of Physical Chemistry Letters **3**, 3264–3270 (2012).

[28]S. Cherevko, T. Reier, A. R. Zeradjanin, Z. Pawolek, P. Strasser, and K. J. J. Mayrhofer, "Stability of nanostructured iridium oxide electrocatalysts during oxygen evolution reaction in acidic environment," Electrochemistry Communications **48**, 81–85 (2014).

[29]T. Binninger, R. Mohamed, K. Waltar, E. Fabbri, P. Levecque, R. Kötz, and T. J. Schmidt, "Thermodynamic explanation of the universal correlation between oxygen evolution activity and corrosion of oxide catalysts," Scientific Reports **5**, 12167 (2015).

[30]K. S. Exner, "On the lattice oxygen evolution mechanism: Avoiding pitfalls," ChemCatChem **n/a**, n/a (2021).

[31]H. Over, "Fundamental studies of planar single-crystalline oxide model electrodes (RuO_2, IrO_2) for acidic water splitting," ACS Catalysis **11**, 8848–8871 (2021).

[32]F. Carrera, F. Torrico, D. T. Richens, A. Muñoz Páez, J. M. Martínez, R. R. Pappalardo, and E. Sánchez Marcos, "Combined experimental and theoretical approach to the study of structure and dynamics of the most inert aqua ion [Ir(H2O)6]3+ in aqueous solution," The Journal of Physical Chemistry B **111**, 8223–8233 (2007).

[33]O. Kasian, J.-P. Grote, S. Geiger, S. Cherevko, and K. J. J. Mayrhofer, "The common intermediates of oxygen evolution and dissolution reactions during water electrolysis on iridium," Angewandte Chemie International Edition **57**, 2488–2491 (2018).

[34]D. Leanza, M. Mirolo, C. A. F. Vaz, P. Novák, and M. El Kazzi, "Surface degradation and chemical electrolyte oxidation induced by the oxygen released from layered oxide cathodes in Li-ion batteries," Batteries & Supercaps **2**, 482–492 (2019).

[35]M. J. N. Pourbaix, J. V. Muylde, and N. de Zoubov, "Electrochemical properties of the platinum metals," Platinum Metals Review **3**, 100–106 (1959).

[36]A. A. Bolzan, C. Fong, B. J. Kennedy, and C. J. Howard, "Structural Studies of Rutile-Type Metal Dioxides," Acta Crystallographica Section B **53**, 373–380 (1997).

[37]M. Bajdich, M. García-Mota, A. Vojvodic, J. K. Nørskov, and A. T. Bell, "Theoretical investigation of the activity of cobalt oxides for the electrochemical oxidation of water," Journal of the American Chemical Society **135**, 13521–13530 (2013).

[38]F. Reikowski, F. Maroun, I. Pacheco, T. Wiegmann, P. Allongue, J. Stettner, and O. M. Magnussen, "Operando surface x-ray diffraction studies of structurally defined Co_3O_4 and CoOOH thin films during oxygen evolution," ACS Catalysis **9**, 3811–3821 (2019).

[39]J. Chivot, L. Mendoza, C. Mansour, T. Pauporté, and M. Cassir, "New insight in the behaviour of Co–H_2O system at 25–150°c, based on revised pourbaix diagrams," Corrosion Science **50**, 62–69 (2008).

[40]R. G. Delaplane, J. A. Ibers, J. R. Ferraro, and J. J. Rush, "Diffraction and spectroscopic studies of the cobaltic acid system $HCoO_2$–$DCoO_2$," The Journal of Chemical Physics **50**, 1920–1927 (1969).